AWARD NUMBER: W81XWH-13-1-0354

TITLE: "Targeting the Adipocyte-Tumor Cell Interaction in Prostate Cancer Treatment"

PRINCIPAL INVESTIGATOR: Jorge Moscat, PhD

CONTRACTING ORGANIZATION:

Sanford-Burnham Medical Research Institute
La Jolla, CA 92037

REPORT DATE: October 2015

TYPE OF REPORT: Annual

PREPARED FOR: U.S. Army Medical Research and Materiel Command
Fort Detrick, Maryland 21702-5012

DISTRIBUTION STATEMENT: Approved for Public Release;
Distribution Unlimited

The views, opinions and/or findings contained in this report are those of the author(s) and should not be construed as an official Department of the Army position, policy or decision unless so designated by other documentation.

REPORT DOCUMENTATION PAGE

Form Approved
OMB No. 0704-0188

Public reporting burden for this collection of information is estimated to average 1 hour per response, including the time for reviewing instructions, searching existing data sources, gathering and maintaining the data needed, and completing and reviewing this collection of information. Send comments regarding this burden estimate or any other aspect of this collection of information, including suggestions for reducing this burden to Department of Defense, Washington Headquarters Services, Directorate for Information Operations and Reports (0704-0188), 1215 Jefferson Davis Highway, Suite 1204, Arlington, VA 22202-4302. Respondents should be aware that notwithstanding any other provision of law, no person shall be subject to any penalty for failing to comply with a collection of information if it does not display a currently valid OMB control number. **PLEASE DO NOT RETURN YOUR FORM TO THE ABOVE ADDRESS.**

1. REPORT DATE	2. REPORT TYPE	3. DATES COVERED
October 2015	Annual	30 Sep 2014- 29 Sep 2015

4. TITLE AND SUBTITLE

"Targeting the Adipocyte-Tumor Cell Interaction in Prostate Cancer Treatment"

5a. CONTRACT NUMBER
W81XWH-13-1-0354

5b. GRANT NUMBER

5c. PROGRAM ELEMENT NUMBER

6. AUTHOR(S)

Jorge Moscat, PhD

E-Mail: jmoscat@sbpdiscovery.org

5d. PROJECT NUMBER

5e. TASK NUMBER

5f. WORK UNIT NUMBER

7. PERFORMING ORGANIZATION NAME(S) AND ADDRESS(ES)

Sanford-Burnham Medical Research Institute
10901 North Torrey
Pines La Jolla, CA 92037

8. PERFORMING ORGANIZATION REPORT NUMBER

9. SPONSORING / MONITORING AGENCY NAME(S) AND ADDRESS(ES)

U.S. Army Medical Research and Materiel Command
Fort Detrick, Maryland 21702-5012

10. SPONSOR/MONITOR'S ACRONYM(S)

11. SPONSOR/MONITOR'S REPORT NUMBER(S)

12. DISTRIBUTION / AVAILABILITY STATEMENT

Approved for Public Release; Distribution Unlimited

13. SUPPLEMENTARY NOTES

14. ABSTRACT

Prostate cancer (PCa) is one of the leading causes of death among men in the United States. Obesity is another growing epidemic health problem in Western societies and in developing nations, and represents one of the greatest threats to global human health. Several epidemiological studies during the last decade have pointed to an association between obesity and increased risk factor for PCa progression and aggressiveness. However, despite the relatively high amount of epidemiological data available, little is known about the molecular basis underlying the association between PCa progression, obesity and inflammation, and the role of the adipocyte-cancer cell interaction in this process. The goal of this project is to test the hypothesis that p62 is a molecular link in the cross-talk between obesity, inflammation and prostate cancer progression. Here, we have generated a new mouse model to address this question. Unveiling the molecular mechanisms governing obesity-induced prostate cancer progression will have a great impact in our understanding of this process, and its relevance for potential more targeted and efficacious therapies in PCa.

15. SUBJECT TERMS

Prostate cancer, obesity, inflammation, p62, metastasis, adipocyte, mouse models

16. SECURITY CLASSIFICATION OF:			17. LIMITATION OF ABSTRACT	18. NUMBER OF PAGES	19a. NAME OF RESPONSIBLE PERSON
					USAMRMC
a. REPORT	b. ABSTRACT	c. THIS PAGE			19b. TELEPHONE NUMBER *(include area code)*
U Unclassified	U Unclassified	U Unclassified	UU Unclassified	45	

Table of Contents

Page

1. Introduction……. 1

2. Keywords……. 1

3. Overall Project Summary……... 1

4. Key Research Accomplishments…… 7

5. Conclusion…… 7

6. Publications, Abstracts, and Presentations…….…..……. 7

7. Inventions, Patents and Licenses…… 8

8. Reportable Outcomes..…… 8

9. Other Achievements…… 8

10. References…… 9

11. Appendices…….. 9

1. INTRODUCTION

Prostate cancer (PCa) is the leading cancer diagnosis and the second-leading cause of death among men in the United States[1]. Obesity is another growing epidemic in Western societies and in developing nations, and represents one of the greatest threats to global human health[2,3]. Importantly, there is emerging support for a positive association between obesity and increased risk of PCa, with stronger links to more aggressive fatal disease[4,5]. However, despite the relatively high amount of epidemiological data available, little is known about the molecular basis underlying the association among PCa progression, obesity, and inflammation, or the role of the adipocyte-cancer cell interaction in this process. Therefore, biochemical and genetic studies using physiologically relevant models that mimic the complexity of these processes are sorely needed. Given the current obesity epidemic, it is urgent to explore possible interventions to disrupt the obesity-PCa link. Identifying the molecular mechanisms governing obesity-induced PCa progression will have a great impact on our understanding of this process, and will help in the design of more targeted and efficacious therapies in PCa. Collaborative efforts between our two laboratories (Diaz-Meco and Moscat) have identified p62 as a novel player in PCa and in obesity-induced inflammation, providing us with a unique in vivo model to study, at a cellular and molecular level, the mechanisms regulating the obesity-PCa interface. Understanding the role of p62 in the cellular and molecular pathways controlling PCa progression in obesity will generate high-impact information critical for the design of new therapeutic strategies aimed at targeting the tumor microenvironment. Interfering with adipocyte-tumor cell interactions to disrupt PCa progression could be a much-needed new therapeutic avenue.

2. KEYWORDS

Prostate cancer; obesity; inflammation; p62; tumor microenvironment; adipocyte; IL-6; mouse models; stroma; mTORC1; nutrient sensing; cachexia.

3. OVERALL PROJECT SUMMARY

This annual report corresponds to the second year of the Synergistic Idea Development Awards W81XWH-13-1-0353 (PI: Dr. Diaz-Meco) and W81XWH-13-1-0354 (Partnering PI: Dr. Moscat).

The goal of this synergistic project is to test the hypothesis that p62 is a molecular link that connects obesity, inflammation, and PCa progression. This will be addressed in three Specific Aims:

Aim 1. Investigate the in vivo role of p62 in the relationship between adipose tissue and PCa progression.

Aim 2. Determine the role of p62-mediated inflammation in the PCa tumor microenvironment.

Aim 3: Explore the role of p62 in the adipocyte-PCa cell interaction through cellular and mechanistic in vitro studies.

The overall progress of the project has been excellent. We have greatly advanced the project and successfully completed an important part of the project. According to the approved SOW we have performed the following tasks corresponding to this period:

Task 1: Breeding of the required mice for experiments (Months 1-16; Diaz-Meco & Moscat). This task has been completed as planned.

Task 1.1. Diaz-Meco lab has bred TRAMP+ mice with $p62^{Adipo}$ mice provided by Moscat lab and generated the required experimental mice. No major problems have been encountered with the breeding of these mice. These mice are now being subjected to analysis in the different tasks.

Task 1.2. Moscat lab has also bred WT, p62 KO, IL-6 KO and p62/IL-6 DKO mice required for the

planned experiments.

Task 2: Analysis of the PCa phenotype of TRAMP^{+}/p62^{Adipo} and TRAMP^{+} mice (Months 4-16; Diaz-Meco)

Task 2.1. Disease-free survival curves (Kaplan-Meier plots) have been completed. No changes in survival were observed comparing the groups of both genotypes (Fig. 1A). This was most probably

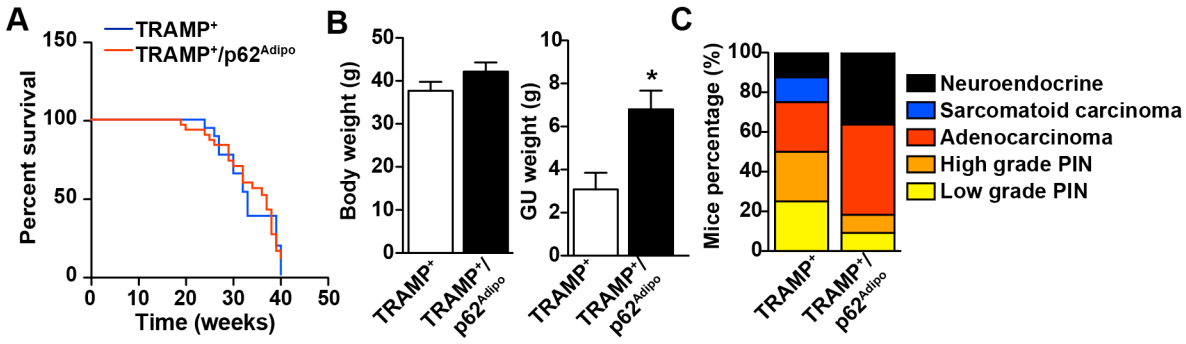

D

Genotype	Metastasis incidence
TRAMP^{+}	28.6% (4/14)
TRAMP^{+}/p62^{Adipo}	36.7% (11/30)

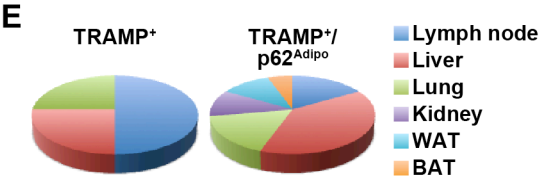

F

Genotype	Site of metastasis					
	Lymph nodes	Liver	Lung	Kidney	WAT	BAT
TRAMP^{+}	14.3% (2/14)	7.1% (1/14)	7.1% (1/14)	0.0% (0/14)	0.0% (0/14)	0.0% (0/14)
TRAMP^{+}/p62^{Adipo}	10.0% (3/30)	23.3% (7/30)	10.0% (3/30)	6.7% (2/30)	6.7% (2/30)	3.3% (1/30)

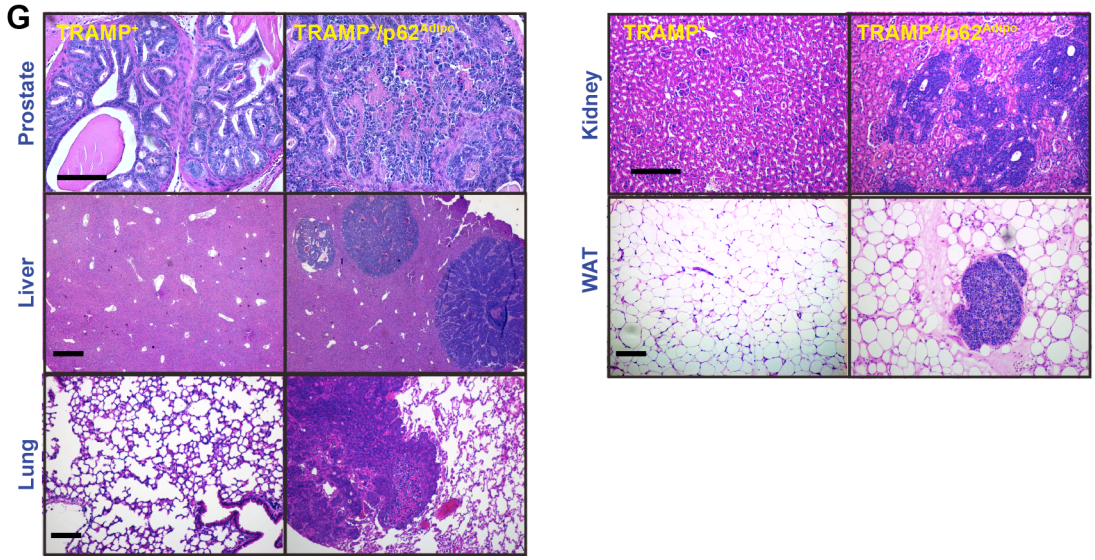

Figure 1. Analysis of the PCa phenotype of TRAMP^{+} and TRAMP^{+}/p62^{Adipo} mice. (**A**) Kaplan-Meier survival curve of TRAMP^{+} (n=20), compared with TRAMP^{+}/p62^{Adipo} (n=31). (**B**) Graph showing body weight and genitourinary (GU) tract weight of TRAMP^{+} (n=10) and TRAMP^{+}/p62^{Adipo} (n=20) mice at 30-40 weeks of age. (**C**) Histological analysis of prostrates of the indicated genotypes. **(D)** Table showing incidence of metastases from TRAMP^{+} (n=14) compared with TRAMP^{+}/p62^{Adipo} mice (n=30). **(E and F)** Pie chart and table showing the distribution of metastasis sites. (**G**) H&E staining of prostates and metastasis in different tissues of the indicated genotypes at 37 weeks of age. Scale bar=100 µm. Results are shown as means ± SEM, *p<0.05.

due to the huge volume of the primary tumor in both groups.

Task 2.2. Analysis of PCa progression in TRAMP^{+}/p62^{Adipo} and TRAMP^{+} mice: Diaz-Meco lab has completed for the most part the characterization of the phenotype of TRAMP^{+}/p62^{Adipo}. We have confirmed and extended to a significant number of mice the preliminary characterization of a limited cohort reported in our first year report. We have completed subtasks 2.2.1 to 2.2.5. The results of these tasks are presented in Fig. 1. Body weight and GU weight was determined at the endpoint of the experiment. Although there was a tendency of higher body weight in the TRAMP^{+}/p62^{Adipo} mice, there were not significant differences in this parameter between both groups (Fig. 1B). This result was unexpected, but suggested that the presence of the tumor could have a profound effect in the whole metabolism of the host. Thus, whereas our previously published results[6] demonstrated that p62^{Adipo} mice are significantly more obese that WT control mice in regular as well as in high-fat diet, however TRAMP^{+}/p62^{Adipo} mice loose weight and their body weight is not significantly different from that of TRAMP^{+} mice. This intriguing result suggested us the possibility that these mice could be suffering cachexia as a result of the PCa tumor. In contrast to body weight, the GU weight was significantly increased in TRAMP^{+}/p62^{Adipo} mice as compared to control group (Fig. 1B). Most importantly, we found that TRAMP^{+}/p62^{Adipo} mice developed a more aggressive PCa phenotype with higher incidence of adenocarcinoma and neuroendocrine tumors than TRAMP^{+} control mice (Figs. 1C). Interestingly, TRAMP^{+}/p62^{Adipo} mice also had a higher metastasis incidence as compared to the control group (Fig. 1D). Of note, there was also a tissue preference for the metastasis in the TRAMP^{+}/p62^{Adipo} mice with increased incidence in liver and lung (Figs. 1E-1G). Furthermore, we also found metastasis in kidney, WAT and BAT in TRAMP^{+}/p62^{Adipo} mice that were not detected in TRAMP^{+} (Figs. 1E-1G). Collectively, these results suggest that the loss of p62 selectively in the adipose tissue drives tumorigenesis and invasiveness in PCa. This is consistent the increased risk associated with more aggressive PCa to obesity found in multiple epidemiological data[7,8]. In addition, these results demonstrate a cause and effect molecular link to start dissecting the mechanism connecting obesity and PCa progression in a suitable, physiologically relevant genetic in vivo model independent of food intake and diet.

Task 3: Analysis of the general metabolic characterization of TRAMP+/p62Adipo and TRAMP+ mice (Months 4-16; Moscat). A cohort of 6 mice of each genotype has been analyzed for metabolic studies (CLAMS and DXA). We have completed subtasks 3.1 to 3.7 and initiated subtask 3.8. The results of these tasks are presented in Fig. 2. As planned in Task 3.1, we monitored the body weight of a large cohort of mice during 10 months. In agreement with our results of Fig. 1B, there was a tendency of higher body weight in the TRAMP^{+}/p62^{Adipo} mice group, however that was not overall significant (Fig. 2A). Furthermore, there were not significant changes in percentage of lean mass or fat mass as determined by body composition (Fig. 2B). Oil red staining to assess lipid accumulation in liver also revealed not significant differences between both genotypes (Fig. 2C). Next, we performed full metabolic characterization by using an automated indirect calorimetry system (CLAMS). The analysis of all the metabolic parameters measured including food intake, drinking, horizontal and vertical activity, volume of O_2 (VO_2), volume of CO_2 (VCO_2), respiratory exchange ratio (RER) and energy expenditure (EE) did not show significance changes between the TRAMP^{+}/p62^{Adipo} mice group as compared to the control TRAMP^{+} mice (Figs. 2D-2L). These surprising results are extremely interesting because they unveiled the impact that the PCa tumor has in the metabolism. As mentioned above in regard to the lack of differences in body weight, these metabolic results suggest that TRAMP^{+}/p62^{Adipo} mice are suffering a cancer-associated cachexia phenotype. In fact, a similar metabolic analysis performed in p62^{Adipo} mice showed decreased energy expenditure accompanied by a significant reduction in locomotor activity as compared to WT control mice[6]. This indicates that the presence of tumor in TRAMP^{+}/p62^{Adipo} mice provoked a metabolic dysfunction in the p62^{Adipo} mice

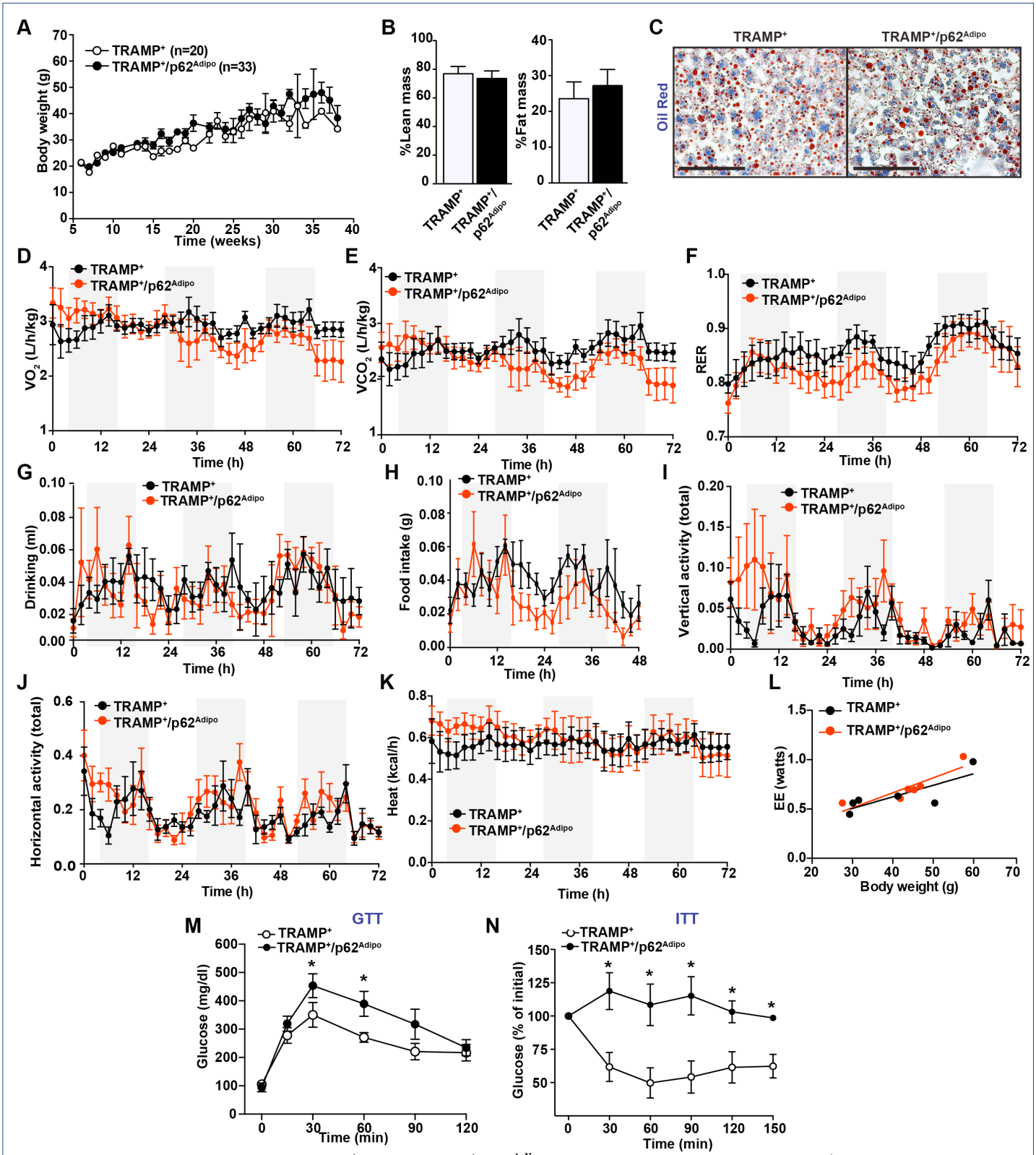

Figure 2. Metabolic analysis of TRAMP^{+} and TRAMP^{+}/p62^{Adipo} mice. (A) Body weight of TRAMP^{+} (n=20), compared with TRAMP^{+}/p62^{Adipo} (n=33) from 6 to 40 weeks of age. **(B)** DEXA analysis of mice of 7 month of age. Fat and lean mass as the percentage of total body weight. **(C)** Representative pictures of Oil Red staining from TRAMP^{+} and TRAMP^{+}/p62^{Adipo} livers. **(D-L)** Mice were housed in a metabolic chamber and monitored using Comprehensive Lab Animal Monitoring System CLAMS. **(D)** Oxygen consumption. **(E)** Carbon Dioxide production. **(F)** Respiratory Exchange Rate. **(E)** Drinking volume. **(H)** Food intake. **(I-J)** Locomotor activity. **(K)** Heat production. **(L)** Energy expenditure in relation to body weight. **(M)** Glucose tolerance and **(N)** insulin sensitivity tests. Scale bar=100 μm.

increasing their metabolic rate to reach the same energy expenditure than TRAMP^{+} mice. This is consistent with the increased energy expenditure and activation of thermogenesis that have been proposed as causative for cancer-associated cachexia [9,10,11]. Of note, TRAMP^{+}/p62^{Adipo} mice that have no longer increased body weight or energy expenditure alterations, they however still displayed an insulin resistance phenotype. Thus, TRAMP^{+}/p62^{Adipo} mice have defects in glucose and insulin responses as measured in glucose tolerance (GTT) and insulin tolerance (ITT) tests (Figs. 2M-2N). These results open a new aspect of investigation in our project, since not only the adipose tissue talks to the tumor to make it more aggressive, but also the tumor impacts the metabolism of the host.

Task 4. Gene expression studies of prostate and metabolic tissues in TRAMP^{+}/p62^{Adipo} and TRAMP mice (Months 12-18; Diaz-Meco & Moscat).

Task 4.1. Determine by Q-PCR in RNA of liver, muscle, white adipose tissue, brown adipose tissue and prostate of mice of the different genotypes. This analysis will be performed to a single time point selected from the results of Task 2 & 3. The following well established metabolic genes will be determined: ACO, ACC, PGC-1α, PGC-1β, CPT-1, UCP1, UCP2, UCP3, G6Pase, PEPCK, PPAR-α, PPAR-δ, PPARγ, C/EBPα, and C/EBPβ. (Moscat).

For this task, we have decided to do RNASeq analysis in the samples of white adipose tissue (WAT) that we believe will be the critical initiator of the crosstalk with the prostate, and to have a more unbiased and complete view of the metabolic changes that could be driving the PCa phenotype that we

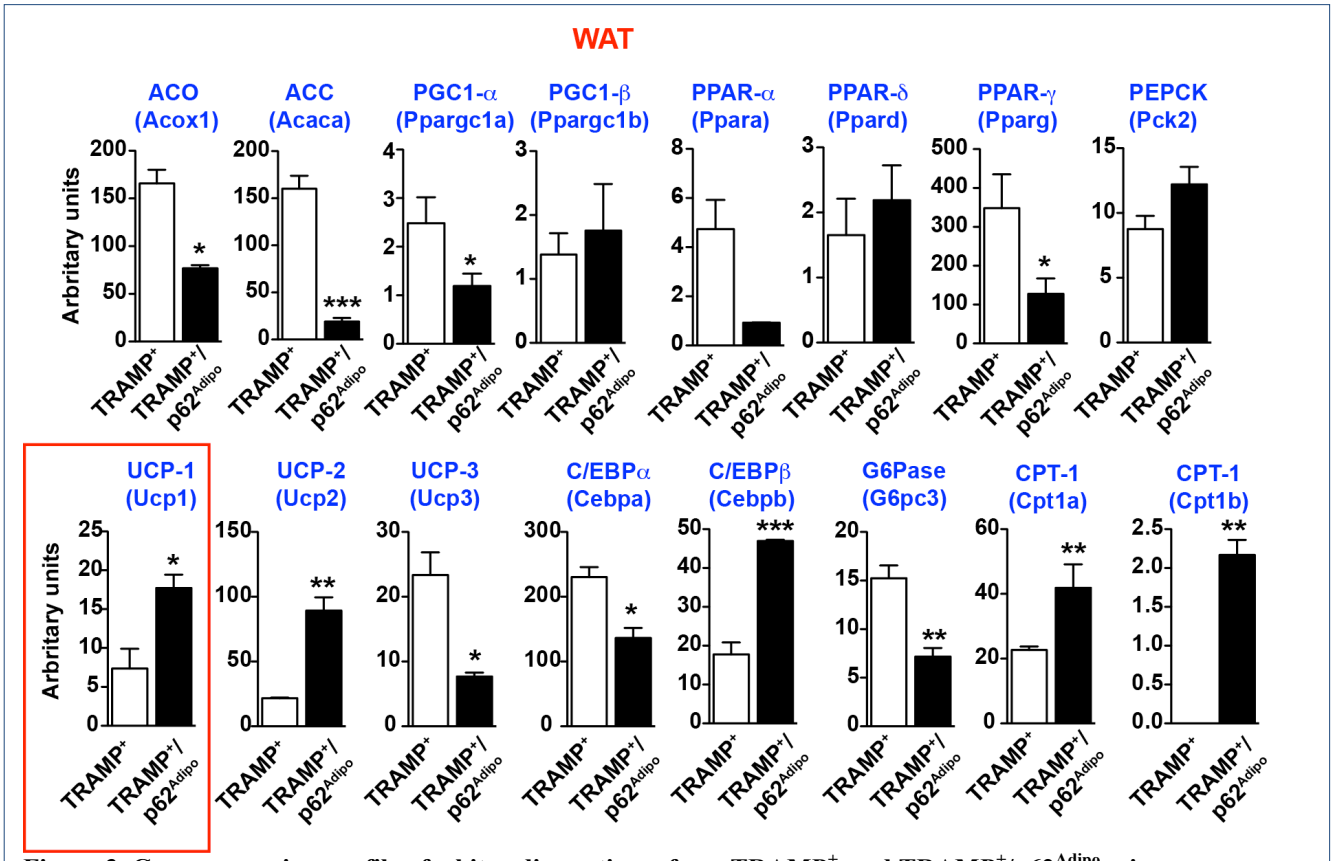

Figure 3. Gene expression profile of white adipose tissue from TRAMP^{+} and TRAMP^{+}/p62^{Adipo} mice.
Q-PCR of metabolic genes (ACO, ACC, PGC-1α, PGC-1β, CPT-1, UCP1, UCP2, UCP3, G6Pase, PEPCK, PPAR-α, PPAR-δ, PPARγ, C/EBPα, and C/EBPβ) in epididymal white adipose tissue from TRAMP^{+} and TRAMP^{+}/p62^{Adipo} mice. Results are shown as means ± SEM. n=3. *p<0.05, **p<0.01, ***p<0.001.

have found in task 2. We have just got the results and they will be thoroughly analyzed during the next period. Initially, we have looked at the metabolic genes that were planed in this task. The results are presented in Fig. 3. The most important finding during this analysis was the switch found in the expression of UCP1 in the WAT of the $TRAMP^{+}/p62^{Adipo}$ mice (Fig. 3). An increase in UCP1 in WAT is known as WAT browning since UCP1 is mostly expressed in brown adipose tissue (BAT). Interestingly, $p62^{Adipo}$ mice had a decreased expression of UCP1 in BAT consistent with their reduced energy expenditure[6], whereas $TRAMP^{+}/p62^{Adipo}$ mice have increase levels of UCP1 in WAT. This is very interesting because it has been recently shown that WAT browning with increased expression of UCP1 takes place in the initial stages of cancer-associated cachexia. Therefore, our gene expression results are totally consistent with the metabolic data obtained in Task 3, and indicated that there is a cancer-associated cachexia phenotype in $TRAMP^{+}/p62^{Adipo}$ mice.

Task 5. Metabolomic profile of PCa tumors and adipose tissue (Months 19-22; Diaz-Meco & Moscat).
This task will be addressed during the next year of the project.

Task 6. In vivo characterization of inflammation in PCa tumors, and adipose tissue (Months 23-30; Diaz-Meco & Moscat).
Task 6.1 that is pending from the previous year will be completed during the next period. The inflammatory characterization of the adipose tissue will be obtained from the RNASeq analysis already performed in task 4.1.

Task 7. 3D Organotypic cultures to study the adipocyte-PCa cell interaction in vitro (Months 30-36; Diaz-Meco & Moscat).
This task will be addressed in the next period.

We believe we have made an excellent progress in the project, and have got very exciting results. During the next year, we will continue working to complete the pending tasks, and to decipher the mechanism how the adipose tissue controls PCa, but also we will interrogate in our model how the PCa tumor talks to the adipose tissue to induce cachexia.

In addition, we have also complemented these studies with research aimed to understand how p62 senses nutrients. These results have been recently published in the top-notch journal **Cell Reports**[12] (see Appendix). The ability to sense and response to fluctuation in nutrient levels is a requisite for life. During food abundance, nutrient sensing pathways engage anabolism and storage, whereas scarcity triggers homeostatic mechanisms, such as the mobilization of internal stores through autophagy. Importantly, nutrient-sensing pathways are commonly deregulated in human metabolic disease such as obesity. Central to this process is the nutrient-sensitive kinase complex mTORC1 that integrate the response to growth factors, energy levels and nutrients, specifically amino acids. Interestingly, we have found a nutrient sensing pathway that is selectively activated in response to amino acids and that is critical for PCa cells. We have identified a kinase cascade that is highly upregulated in PCa and that is essential for tumor development. Because kinases are eminently druggable targets, our findings have the potential to open new avenues for designing novel treatments for cancer.

4. KEY RESEARCH ACCOMPLISHMENTS

- p62 selective deficiency in the adipose tissue promotes a more aggressive PCa phenotype, providing a link between obesity and adiposity and PCa progression.
- p62 selective deficiency in the adipose tissue changes the metastasis incidence and the tissue preference for metastasis.
- Generation of a new mouse model to study cancer-associated cachexia.
- Full metabolic characterization of mice with selective deficient of p62 in the adipose tissue and PCa tumors revealed a phenotype of cancer-associated cachexia.
- p62 selective deficiency in the adipose tissue promotes a WAT switch with browning and increased UCP1.
- Identification of a novel kinase cascade that regulates nutrient sensing to control mTORC1 activation.
- Novel nutrient sensing mechanism critical for PCa cell growth and autophagy.
- The p62-kinase cascade identified is overexpressed in human PCa tumors and is required for PCa tumor growth.

5. CONCLUSION

During this year, there have been three major areas of effort of this synergistic project:

1) The full characterization of the prostate phenotype caused in vivo by p62 selective deficiency in the adipose tissue that has lead to the important conclusion that obesity drives a more aggressive PCa phenotype with higher incidence of metastasis.
2) The metabolic studies at whole body level as well as a cellular level that have identified a cancer-associated cachexia phenotype in the obese p62 adipose-deficient mice harboring PCa tumors. This opens the need to investigate not only how the adipose tissue influences the PCa tumor, but also how the tumor instructs and transforms the adipose tissue for its own benefit.
3) The complementary studies at understanding the molecular mechanisms how p62 senses nutrients that have allowed the identification of a druggable kinase cascade as potential novel therapeutic strategies for PCa.

6. PUBLICATIONS, ABSTRACTS, AND PRESENTATIONS

Publications:

✓ Peer-Reviewed Scientific Journals:

Linares J.F., Duran A., Reina-Campos M., Aza-Blanc P., Campos A., Moscat J., Diaz-Meco M.T. (2015). Amino Acid Activation of mTORC1 by a PB1-Domain-Driven Kinase Complex Cascade. **Cell Rep.** 12, 1339-52. PMCID: PMC4551582

Moscat J., Richardson A., Diaz-Meco M.T. (2015). Nutrient stress revamps cancer cell metabolism. **Cell Research** 25:537-38.

✓ Lay press:

Our publication in Cell Reports has been reviewed in several lay articles:

Health Innovations. August 14, 2015. "Study identifies mTOR pathway that controls cancer proliferation via nutrients".

Science Daily. August 13, 2015. "Scientists discover a pathway that controls cancer cell proliferation by nutrients".

Abstracts and presentations:

"Metabolic Reprogramming in the Tumor Stroma by the p62/mTORC1 Pathway" Case Western Reserve, Cleveland, 2014. Speaker (Moscat).

"Autophagy and Metabolic Reprograming in the Tumor Stroma" in the Major Symposium on "Autophagy and Cancer" at the Annual AACR meeting, Philadelphia, 2015. Speaker (Moscat).

"Dual role of p62/mTORC1 in the tumor microenvironment". The San Diego Center for Systems Biology. UCSD (San Diego, 2015). Speaker (Moscat).

"Metabolic reprograming in cancer" C3 Cancer Centers Consortium Retreat, UCSD, 2015. Speaker (Moscat).

"Targeting Metabolic Reprograming in Cancer" Centro Nacional de Biotecnologia, Madrid, Spain, 2015. Speaker (Moscat)

"Cell Death and Survival Networks". Helmholtz Zentrum München, Munich, 2015 Speaker (Moscat)

"Nutrient Sensing in Cancer". Helmholtz Zentrum München, Munich, 2015 Speaker (Diaz-Meco)

"Metabolic reprograming of the tumor microenvironment through p62". 2nd Annual Meeting of International Ovarian Cancer Consortium in conjunction with the International Symposium on Tumor Microenvironment and Therapy Resistance –Oklahoma City, 2015, Speaker (Diaz-Meco)

7. INVENTIONS, PATENTS AND LICENSES

Nothing to report.

8. REPORTABLE OUTCOMES

- New mouse model to study the link of obesity and prostate cancer and cachexia.
- Two manuscripts (one in Cell Reports and another in Cell Research) co-authored by both laboratories (Moscat and Diaz-Meco) (see above in Publications).

9. OTHER ACHIEVEMENTS

Nothing to report.

10. REFERENCES

1. Society, A.C. Cancer Facts and Figures 2012. *The Amercian Cancer Society* ((2012)).
2. Finkelstein, E.A., Ruhm, C.J. & Kosa, K.M. Economic causes and consequences of obesity. *Annual review of public health* **26**, 239-257 (2005).
3. Finkelstein, E.A. How big of a problem is obesity? *Surg Obes Relat Dis* **10**, 569-570 (2014).
4. Wright, M.E.*, et al.* Prospective study of adiposity and weight change in relation to prostate cancer incidence and mortality. *Cancer* **109**, 675-684 (2007).
5. Mondul, A.M., Giovannucci, E. & Platz, E.A. A prospective study of obesity, and the incidence and progression of lower urinary tract symptoms. *J Urol* **191**, 715-721 (2014).
6. Muller, T.D.*, et al.* p62 links beta-adrenergic input to mitochondrial function and thermogenesis. *The Journal of clinical investigation* **123**, 469-478 (2013).
7. Joshu, C.E.*, et al.* Weight gain is associated with an increased risk of prostate cancer recurrence after prostatectomy in the PSA era. *Cancer Prev Res (Phila)* **4**, 544-551 (2011).
8. Haque, R.*, et al.* Association of body mass index and prostate cancer mortality. *Obesity research & clinical practice* **8**, e374-381 (2014).
9. Blum, D.*, et al.* Cancer cachexia: a systematic literature review of items and domains associated with involuntary weight loss in cancer. *Crit Rev Oncol Hematol* **80**, 114-144 (2011).
10. Tsoli, M.*, et al.* Activation of thermogenesis in brown adipose tissue and dysregulated lipid metabolism associated with cancer cachexia in mice. *Cancer Res* **72**, 4372-4382 (2012).
11. Petruzzelli, M.*, et al.* A switch from white to brown fat increases energy expenditure in cancer-associated cachexia. *Cell Metab* **20**, 433-447 (2014).
12. Linares, J.F.*, et al.* Amino Acid Activation of mTORC1 by a PB1-Domain-Driven Kinase Complex Cascade. *Cell reports* **12**, 1339-1352 (2015).

11. APPENDICES

Publications:

Linares J.F., Duran A., Reina-Campos M., Aza-Blanc P., Campos A., Moscat J., Diaz-Meco M.T. (2015). Amino Acid Activation of mTORC1 by a PB1-Domain-Driven Kinase Complex Cascade. **Cell Rep.** 12, 1339-52. PMCID: PMC4551582.

Moscat J., Richardson A., Diaz-Meco M.T. (2015). Nutrient stress revamps cancer cell metabolism. **Cell Research** 25:537-38.

Article

Cell Reports

Amino Acid Activation of mTORC1 by a PB1-Domain-Driven Kinase Complex Cascade

Graphical Abstract

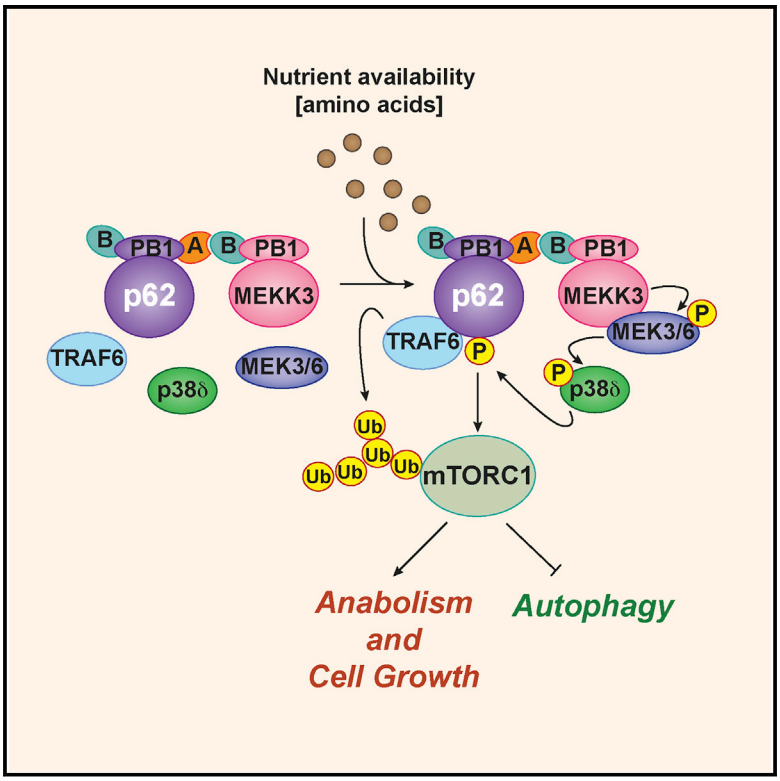

Highlights

- p62 is phosphorylated in response to amino acids by p38δ in a MEKK3-dependent manner
- p62 phosphorylation recruits TRAF6 and promotes mTORC1 translocation to lysosomes
- p38δ-mediated p62 phosphorylation is required for mTORC1 activation by amino acids
- The MEKK3/p38δ kinase cascade modulates autophagy and cancer growth via mTORC1

Authors

Juan F. Linares, Angeles Duran, Miguel Reina-Campos, ..., Alex Campos, Jorge Moscat, Maria T. Diaz-Meco

Correspondence

mdmeco@sbpdiscovery.org

In Brief

Linares et al. identify a kinase cascade that regulates the phosphorylation of the signal adaptor p62 in response to amino acids to control mTORC1 activation. This nutrient-sensing mechanism is relevant for autophagy regulation and tumor growth.

Linares et al., 2015, Cell Reports *12*, 1339–1352
August 25, 2015 ©2015 The Authors
http://dx.doi.org/10.1016/j.celrep.2015.07.045

CellPress

Cell Reports
Article

OPEN ACCESS
CellPress

Amino Acid Activation of mTORC1 by a PB1-Domain-Driven Kinase Complex Cascade

Juan F. Linares,[1] Angeles Duran,[1] Miguel Reina-Campos,[1] Pedro Aza-Blanc,[2] Alex Campos,[3] Jorge Moscat,[1] and Maria T. Diaz-Meco[1,*]
[1]Cell Death and Survival Networks Program
[2]Functional Genomics Core
[3]Proteomics Facility
Sanford Burnham Prebys Medical Discovery Institute, 10901 N. Torrey Pines Road, La Jolla, CA 92037, USA
*Correspondence: mdmeco@sbpdiscovery.org
http://dx.doi.org/10.1016/j.celrep.2015.07.045
This is an open access article under the CC BY-NC-ND license (http://creativecommons.org/licenses/by-nc-nd/4.0/).

SUMMARY

The mTORC1 complex is central to the cellular response to changes in nutrient availability. The signaling adaptor p62 contributes to mTORC1 activation in response to amino acids and interacts with TRAF6, which is required for the translocation of mTORC1 to the lysosome and the subsequent K63 polyubiquitination and activation of mTOR. However, the signal initiating these p62-driven processes was previously unknown. Here, we show that p62 is phosphorylated via a cascade that includes MEK3/6 and p38δ and is driven by the PB1-containing kinase MEKK3. This phosphorylation results in the recruitment of TRAF6 to p62, the ubiquitination and activation of mTOR, and the regulation of autophagy and cell proliferation. Genetic inactivation of MEKK3 or p38δ mimics that of p62 in that it leads to inhibited growth of PTEN-deficient prostate organoids. Analysis of human prostate cancer samples showed upregulation of these three components of the pathway, which correlated with enhanced mTORC1 activation.

INTRODUCTION

Cell metabolism is responsive to the availability of environmental and intracellular nutrients. The mTORC1 kinase complex is a key nutrient sensor and an essential mediator of this response via its actions as a regulator of anabolism and autophagy (Hay and Sonenberg, 2004; Laplante and Sabatini, 2012). The aberrant activation of mTORC1 has important repercussions in several diseases, including cancer (Guertin and Sabatini, 2007; Laplante and Sabatini, 2012; Sabatini, 2006). An essential step in amino-acid-induced activation of mTORC1 is its translocation to the lysosome, mediated by the Rag guanosine triphosphatases (GTPases), where it is activated by another GTPase termed Rheb (Durán and Hall, 2012; Sancak et al., 2008, 2010; Yuan et al., 2013). A lysosomal pentameric complex termed ragulator, along with the vacuolar-ATPase, have been proposed to promote the exchange of GDP for GTP on RagA or RagB in amino-acid-activated cells (Sancak et al., 2010). Additionally, the Rags have been shown to be regulated by other proteins including the GATOR1 complex (Bar-Peled et al., 2013), FLCN (Petit et al., 2013; Tsun et al., 2013), and sestrins (Budanov and Karin, 2008; Chantranupong et al., 2014). There is also evidence for Rag-independent mechanisms of mTORC1 activation. For example, it has recently been reported that Rab1A mediates mTORC1 activity in a Rag-independent manner through the formation of a Rheb-mTORC1 complex in the Golgi (Thomas et al., 2014). Moreover, RagA-null cells display a diffuse cytosolic localization of mTOR and RagC but can, nonetheless, maintain the activity of mTORC1 (Efeyan et al., 2014). Also, it has recently been shown that RheB-null cells retain significant levels of mTORC1 activity (Groenewoud et al., 2013). Moreover, very recent results suggest that the mechanism whereby glutamine activates mTORC1 differs from that of leucine as it is independent of the Rag-Ragulator cascade and is mediated by Arf-1 (Jewell et al., 2015). Therefore, it is clear that our comprehension of mTORC1 activation is still fragmentary and that more work is necessary to achieve a thorough understanding of the mechanisms that modulate its activity in response to nutrients.

The signaling adaptor p62 (also known as SQSTM1) is central to cell survival and proliferation through the activation of mTORC1 (Duran et al., 2008, 2011; Linares et al., 2013; Moscat and Diaz-Meco, 2009, 2011; Valencia et al., 2014). This is achieved through the interaction of p62 with raptor, a distinctive component of the mTORC1 complex, and by facilitating mTORC1 translocation to the lysosome, a process that likely involves the interaction of p62 with the Rag proteins (Duran et al., 2011). Our recent data demonstrate that the E3-ubiquitin ligase TRAF6 is another important player in this process (Linares et al., 2013). That is, the interaction of TRAF6 with p62 facilitates the lysosomal recruitment of mTORC1 and catalyzes the K63 polyubiquitination of the mTOR subunit of the complex, which is required for its optimal activation by amino acids (Linares et al., 2013). Therefore, the p62/TRAF6 tandem must be considered an important modulator of nutrient sensing through mTORC1. Consistent with this notion, the loss of TRAF6, like that of p62, attenuated proliferation and the transforming properties of cancer cells and led to enhanced autophagy, which could be rescued by the expression of a permanently active RagB mutant, indicating that p62 acts upstream of the Rag proteins

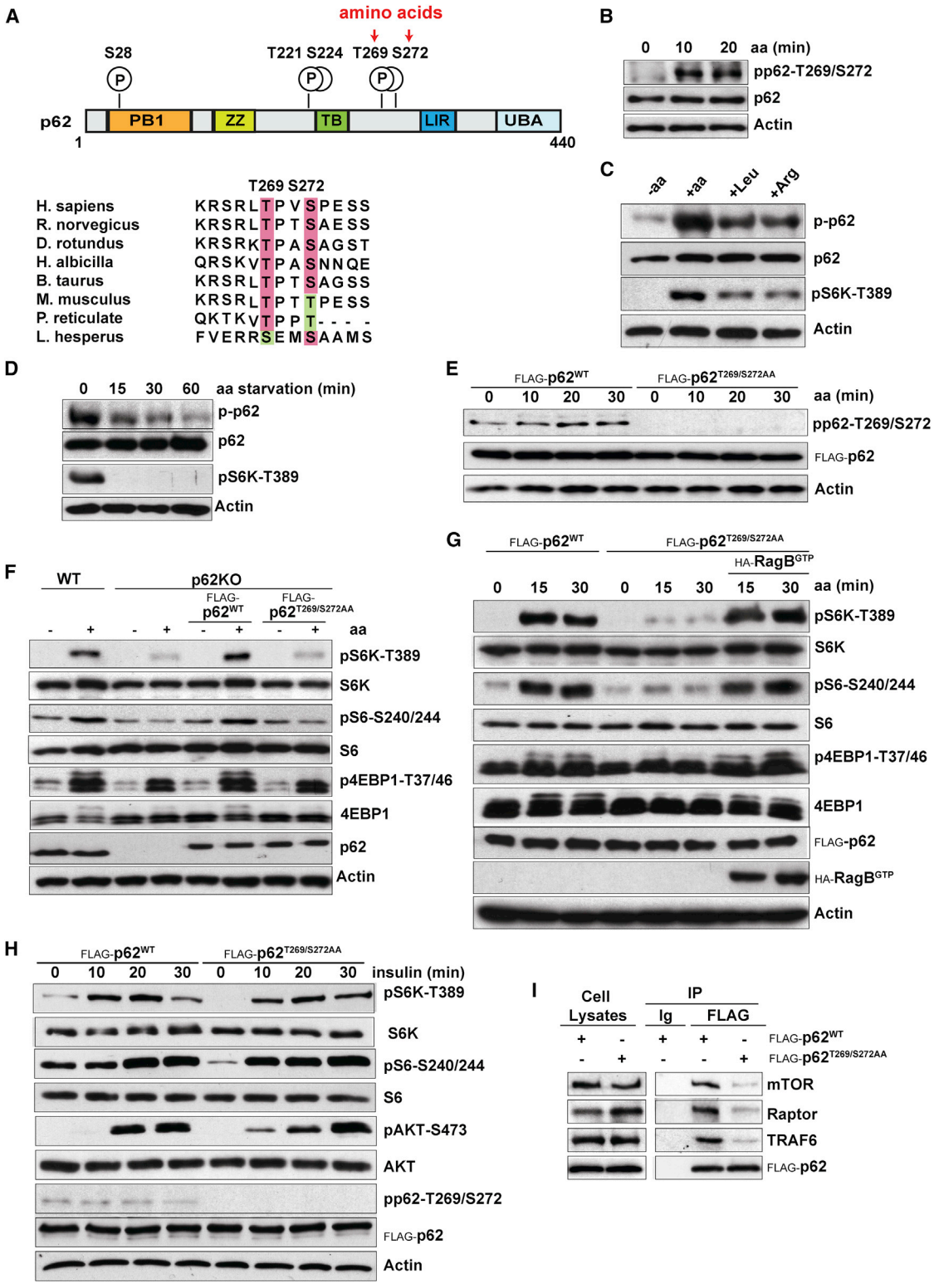

Figure 1. p62 Phosphorylation at T269/S272 Was Required for mTORC1 Activation in Response to Amino Acids

(A) p62 domain organization and phosphorylation sites identified by mass spec. Phosphorylation of T269 and S272 was induced by amino acids (upper panel). Alignment of the amino acid sequence of human p62 (264–276) with orthologs in other species is shown (lower panel).

(B) p62 phosphorylation at T269 and S272 is induced by amino acids. HEK293T cells were starved of amino acids for 50 min and restimulated with amino acids for the indicated durations. Cell lysates were analyzed by immunoblotting.

(legend continued on next page)

(Linares et al., 2013). Thus, p62 acts as a scaffold, bringing components involved in the control of mTORC1 signaling to the correct cellular location (Duran et al., 2011). How mTORC1 is linked to the upstream nutrient-sensing machinery and the potential role of p62 in that process are key unresolved issues.

Here, we demonstrate that p62 phosphorylation at T269/S272 is a critical event in channeling the amino acid response to mTORC1 activation, likely due to its ability to orchestrate the binding of p62 with the different components of the mTORC1-signaling complex. That is, we found that p62 organizes a molecular platform with a kinase cascade that is initiated by MEKK3 and triggers the activation of p38δ, is driven by PB1-domain interactions between p62 and MEKK3, and is located on the lysosomal surface. These kinases, like p62, are selectively required for amino-acid-induced mTORC1 activation whereas dispensable for insulin signaling and are required for effective control of cell growth, autophagy, and transformation. These findings define a critical mechanism to transmit nutrient-sensing signals to the mTORC1 complex, which is mediated by phosphorylation of the scaffold protein p62.

RESULTS

p62 Phosphorylation Is Required for the Activation of mTORC1 by Amino Acids

The mechanisms whereby mTORC1 respond to amino acids are not fully understood. Our previous data demonstrated that p62 is a scaffold in this pathway (Duran et al., 2011; Linares et al., 2013), but the process by which it senses amino acids remains to be elucidated. Recent studies have suggested phosphorylation as a regulatory mechanism for the control of p62 function (Ichimura et al., 2013; Linares et al., 2011; Matsumoto et al., 2011). Therefore, we hypothesized that nutrient-driven p62 phosphorylation might underlie p62-mediated activation of mTORC1 in response to amino acids. To address this possibility, we generated HEK293T cells stably expressing FLAG-tagged p62 or FLAG control. Cells were stimulated with amino acids, after which anti-FLAG immunoprecipitates were subjected to liquid chromatography coupled to mass spectrometry (LC-MS). We found that p62 exhibited low-abundance baseline phosphorylation at residues S28, T221, and S224 that was constitutive and not changed upon amino acid stimulation (Figure 1A, upper panel). In contrast, we found that phosphorylation at residues T269 and S272 was markedly induced by amino acids (Figure 1A, upper panel). These sites, and their surrounding sequences, were highly conserved across species (Figure 1A, lower panel). To establish the relevance of these phosphorylation events in mTORC1 signaling, we used a phosphospecific antibody generated against the human p62 peptide SRLT(P)PVS(P)PES(C), which allowed us to detect phospho-T269/S272. Interestingly, immunoblot analysis revealed the strong phosphorylation of p62 at T269/S272 upon re-addition of all amino acids to cells amino acid starved (Figure 1B). Leucine and arginine, two key amino acids for mTORC1 stimulation, also promoted p62-T269/S272 phosphorylation, which correlated with the magnitude of mTORC1 activation, as measured by phosphorylation of S6K (Figure 1C). Conversely, amino acid starvation resulted in a pronounced inhibition of p62-T269/S272 phosphorylation, concomitant with the decrease of mTORC1 activity (Figure 1D). Mutation of p62-T269/S272 sites to alanine ($p62^{T269/S272AA}$) abolished amino-acid-induced p62 phosphorylation, demonstrating that these are bona fide nutrient-sensitive p62 phosphorylation residues (Figure 1E). To explore whether phosphorylation of p62 has any impact on its ability to regulate mTORC1 activity, we used p62 KO MEFs reconstituted with either $p62^{WT}$ or $p62^{T269/S272AA}$. Consistent with our previously published data, mTORC1 activation in response to amino acids was impaired in p62-deficient cells (Figure 1F) (Duran et al., 2011). Importantly, whereas re-expression of $p62^{WT}$ restored mTORC1 activity in the KO MEFs, that of $p62^{T269/S272AA}$ failed to do so, as demonstrated by phosphorylation of multiple mTORC1 downstream targets including S6K, S6, and 4EBP1 (Figure 1F). Furthermore, overexpression of an active RagB-GTP-bound mutant rescued the mTORC1 inhibition caused by $p62^{T269/S272AA}$ expression (Figure 1G). This is in agreement with p62 acting upstream of the Rag GTPases in the control of mTORC1 signaling in the amino acid pathway and supports the notion that p62 phosphorylation also lies upstream of Rag activation (Duran et al., 2011). In keeping with a specific role for p62 in the amino acid, but not in the insulin pathway, insulin did not promote p62 phosphorylation, which, in turn, was not required for insulin-induced mTORC1 activity (Figure 1H). Notably, p62 phosphorylation was also critical for assembly of the amino-acid-induced p62-mTORC1 complex, as demonstrated by the ability of $p62^{T269/S272AA}$ expression to inhibit the interaction of p62 with the different components of mTORC1,

(C) p62 phosphorylation was determined in response to different amino acids. HEK293T cells were starved of amino acids and restimulated with the indicated amino acids for 30 min.

(D) Amino acid starvation inhibits p62 phosphorylation and mTORC1 activation. HEK293T cells were starved of amino acids for the indicated durations. Total cell lysates were analyzed by immunoblotting.

(E) Mutation of p62-T269/S272 sites to alanine ($p62^{T269/S272AA}$) abolished p62 phosphorylation in response to amino acids. HEK293T cells stably expressing FLAG-$p62^{WT}$ or FLAG-$p62^{T269/S272AA}$ were treated and analyzed as in (B).

(F) The $p62^{T269/S272AA}$ mutant was not able to reconstitute mTOR activation in p62KO MEFs. WT and p62KO MEFs, reconstituted with $p62^{WT}$ or $p62^{T269/S272AA}$, were treated as in (B). Cell lysates were analyzed by western blot.

(G) $RagB^{GTP}$ overexpression rescued the defects in mTOR activation by amino acids in cells stably expressing the $p62^{T269/S272AA}$ mutant. HEK293T cells stably expressing FLAG-$p62^{WT}$, FLAG-$p62^{T269/S272AA}$, or FLAG-$p62^{T269/S272AA}$ and FLAG-$RagB^{GTP}$ were treated as in (B) and immunoblotted for the specified proteins.

(H) p62 phosphorylation was not required for mTOR activation by insulin. HEK293T cells stably expressing FLAG-$p62^{WT}$ or FLAG-$p62^{T269/S272AA}$ were deprived of serum for 24 hr and stimulated with insulin for the indicated durations. Cell lysates were analyzed by western blot.

(I) The $p62^{T269/S272AA}$ mutant eliminated the interaction of p62 with different components of the mTORC1 complex. HEK293T cells stably expressing FLAG-$p62^{WT}$ or FLAG-$p62^{T269/S272AA}$ were treated as in (B). Cell lysates and FLAG-tagged immunoprecipitates were immunoblotted to detect the indicated proteins.

Results are representative of three experiments. See also Figure S1.

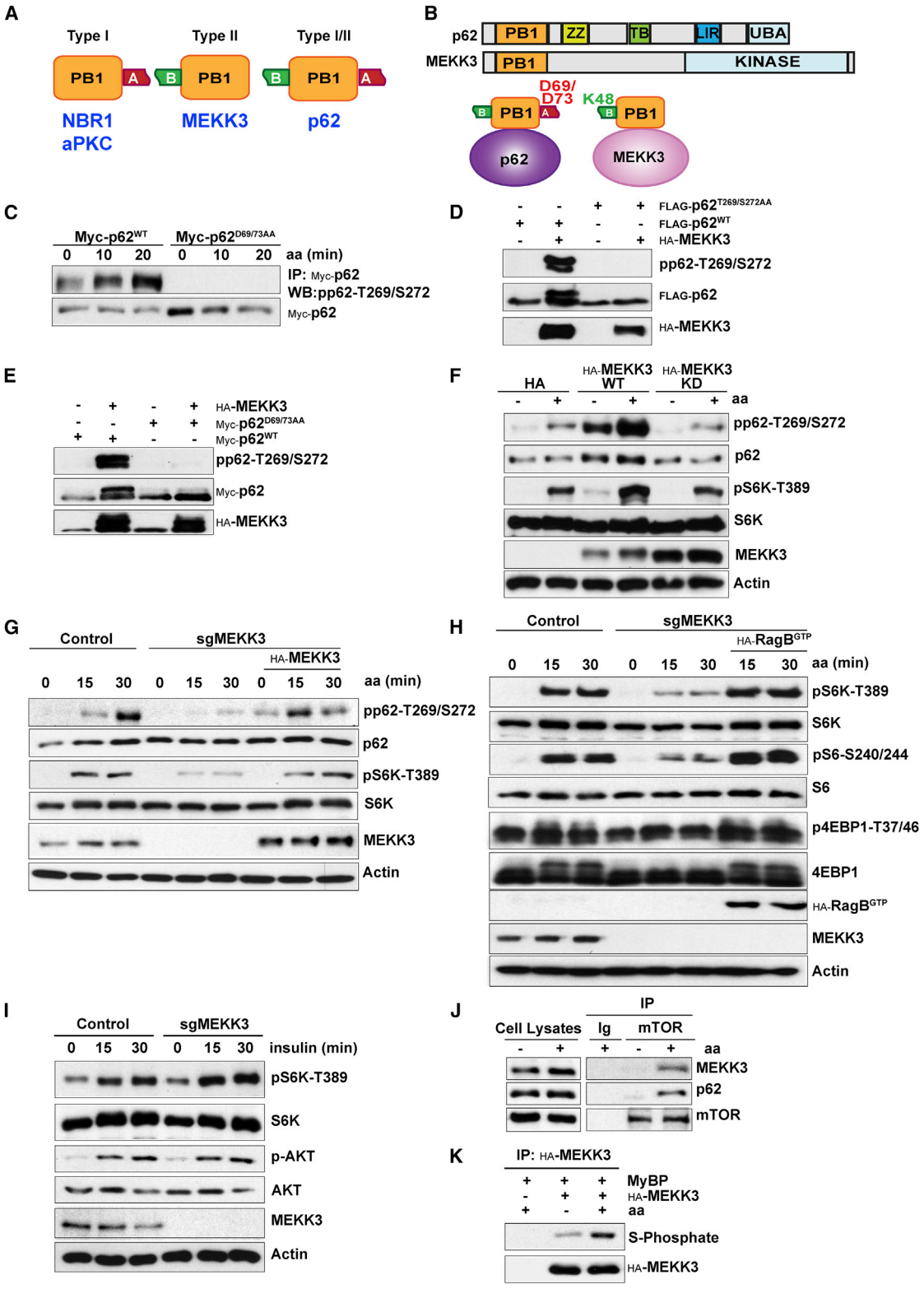

Figure 2. MEKK3 Was a Critical Kinase for p62 Phosphorylation and mTORC1 Activation in Response to Amino Acids

(A) Schematic of the different types of PB1 domains based on the presence of an acid cluster (type I), basic cluster (type II), or both in the same domain (type I/II).

(B) p62 and MEKK3 domain architecture and schematic of the interaction between the acidic cluster of the PB1 domain of p62 and the basic domain of MEKK3.

(legend continued on next page)

including mTOR, raptor, and TRAF6 (Figure 1I). Mutation of p62-T269/S272 sites to aspartic acid did not mimic p62 phosphorylation and did not restore mTORC1 activation or TRAF6 recruitment (Figures S1A and S1B). Together, these findings demonstrate that p62 phosphorylation is a key event in mTORC1 activation, selectively in response to amino acids.

MEKK3 Is a Critical Kinase for Amino-Acid-Induced p62 Phosphorylation

An important question arising from these results is the identity of the amino-acid-activated p62 kinase. In this regard, the structure of p62 includes a PB1 domain, which is a protein-protein interaction module that is present in kinases, such as the atypical PKCs (PKCζ and PKCλ/ι) and MEKK3, as well as in signaling adapters such as Par-6 and NBR1 (Moscat et al., 2006; Sanchez et al., 1998). Protein dimerization occurs by PB1-PB1 interactions through a β-grasp topology in a front-to-back orientation of the two PB1 domains. This involves electrostatic interactions of a cluster of basic residues in one of the PB1 domains that can bind clusters of acidic amino acids in the back of a second PB1 (Figure 2A) (Moscat et al., 2006; Sumimoto et al., 2007). The PB1 domains can be classified into three different types based on the presence of the acid cluster (type I), the basic cluster (type II), or both in the same domain (type I/II; Figure 2A). The PB1 domain of p62 belongs to the type I/II group and, therefore, can accommodate interactions through both faces (Moscat et al., 2006; Sumimoto et al., 2007). In this regard, we previously showed that proteins such as PKCζ, PKCλ/ι, or NBR1, which interact with p62 through its basic cluster, were not required for the activation of mTORC1 (Duran et al., 2011). In contrast, we found that disruption of the acidic cluster of p62, by mutation of D69/D73 to alanine, abolished p62 phosphorylation in response to amino acids (Figures 2B and 2C). This suggests that, if a PB1-domain protein is involved in mTORC1 activation, it must interact with the acidic cluster of p62 using its basic cluster. Interestingly, the PB1-domain-containing kinase, MEKK3, harbors a type II PB1 domain and previous results have shown that the p62 D69A/D73A PB1-domain mutant is unable to interact with MEKK3 (Figure 2B) (Nakamura et al., 2010). Consistent with this, the overexpression of MEKK3 resulted in the phosphorylation of $p62^{WT}$, but not of $p62^{T269/S272AA}$ (Figure 2D). Furthermore, p62 phosphorylation in response to MEKK3 overexpression was eliminated in the p62 PB1-domain mutant (Figure 2E). MEKK3 overexpression, but not that of a kinase-dead mutant, was able to induce the phosphorylation of p62 at T269/S272 (Figure 2F), which correlated with mTORC1 activation (Figure 2F), suggesting that MEKK3 could be a bona fide regulator of p62 phosphorylation and mTORC1 activity. Next, we determined whether MEKK3 is required for mTORC1 activation by using the clustered regularly interspaced short palindromic repeats (CRISPR/Cas9) system to generate MEKK3-deficient HEK293T cells. Notably, the loss of MEKK3 severely reduced p62 phosphorylation and mTORC1 activation in response to amino acids, which were both rescued by the ectopic expression of MEKK3 (Figure 2G). Similar results were obtained with two independent sgMEKK3 clones, as well as by knocking down MEKK3 with a shRNA lentiviral vector in HEK293T, A549, and PC3 cells (Figures S2A–S2D). Of note, the effects of MEKK3 deficiency in mTORC1 activation were rescued by expression of active RagB (Figure 2H). The loss of MEKK3 did not affect insulin-activated mTORC1, consistent with the specificity of p62 in the amino acid pathway (Figure 2I). In keeping with the importance of MEKK3 in this process, we found that, upon cell stimulation by amino acids, endogenous MEKK3 was recruited to an endogenous complex containing p62 and mTOR (Figure 2J). In addition, Figure 2K demonstrates that the kinase activity of MEKK3 was stimulated in amino-acid-treated cells. Collectively, these results demonstrate that p62 is phosphorylated in response to amino acids through a MEKK3-dependent mechanism that is critical for mTORC1 activation and is mediated by the interaction of p62 and MEKK3 through their respective PB1 domains.

MEK3/6 and p38δ Channel MEKK3-Induced Phosphorylation of p62 by Amino Acids

Based on these results, it is possible that p62 could be targeted directly by MEKK3. However, when bacterially expressed

(C) Mutation of p62-D69/73 sites to alanine ($p62^{D69/73AA}$) abolished p62 phosphorylation. HEK293T cells transfected with the indicated plasmids were starved of amino acids for 50 min and restimulated with amino acids for the indicated durations. Myc-tagged immunoprecipitates were analyzed by western blot.
(D) MEKK3 promoted p62 phosphorylation at T269/S272. HEK293T cells were transfected with the indicated plasmids, and cell lysates were analyzed by western blot.
(E) MEKK3-induced p62 phosphorylation required the PB1 domain of p62. HEK293T cells were transfected with the indicated plasmids, and cell lysates were immunoblotted to detect the specified proteins.
(F) Overexpression of MEKK3, but not that of MEKK3 kinase-dead mutant, induced p62 phosphorylation and mTORC1 activation by amino acids. HEK293T cells transfected with the indicated plasmids were deprived of amino acids for 50 min and stimulated with amino acids for 15 min. Cells were analyzed by western blot.
(G) MEKK3 expression rescued p62 phosphorylation and mTOR activation in MEKK3-deficient cells. MEKK3-deficient HEK293T cells generated with the CRISPR/CAS9 system were reconstituted with MEKK3. Cells were deprived of amino acids for 50 min and then stimulated with amino acids for the indicated durations. Cell lysates were immunoblotted for the specified proteins.
(H) $RagB^{GTP}$ overexpression rescued mTOR activation by amino acids in MEKK3-deficient cells. Control and MEKK3-deficient HEK293T cells expressing FLAG-$RagB^{GTP}$ were treated as in (G) and immunoblotted to detect the specified proteins.
(I) MEKK3 was not required for mTOR activation by insulin. Control and MEKK3-deficient HEK293T cells were deprived of serum for 24 hr and stimulated with insulin for the indicated durations. Cell lysates were analyzed by western blot.
(J) MEKK3 is a component of the mTORC1 complex. mTOR immunoprecipitates and cell lysates from HEK293T cells, treated as in (F), were immunoblotted for the indicated proteins.
(K) MEKK3 kinase activity was activated upon amino acid stimulation. HEK293T cells transfected with the indicated plasmids were treated as in (F). HA-tagged immunoprecipitates were used in an in vitro phosphorylation with ATPγS, with myelin basic protein (MyBP) as the substrate, followed by PNBM alkylation and immunoblotting to detect the indicated proteins.
Results are representative of three experiments. See also Figure S2.

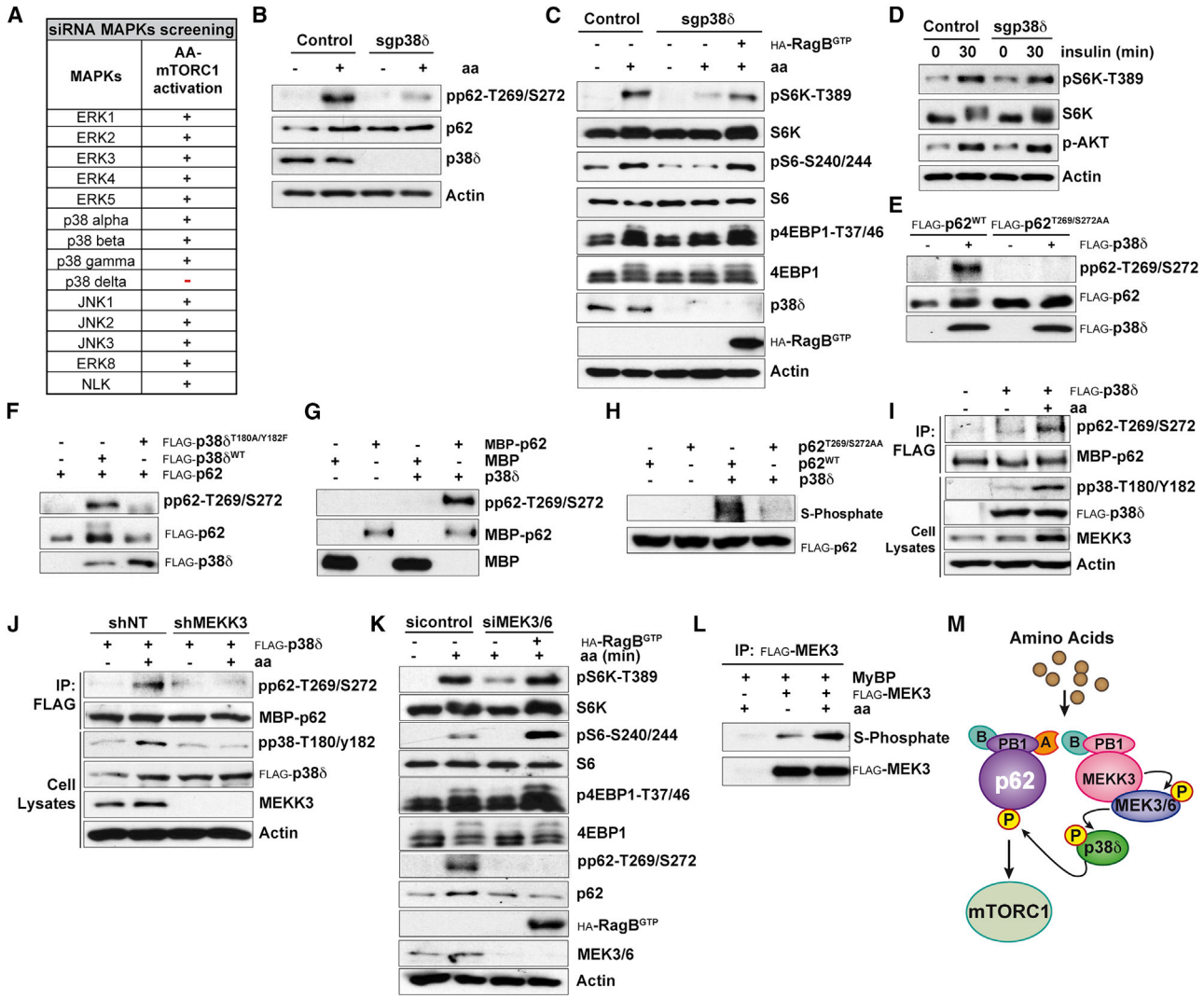

Figure 3. MEKK3/MEK3/6-p38δ Induced p62 Phosphorylation in Response to Amino Acids

(A) p38δ was required for mTORC1 activation in response to amino acids. Results of siRNA screening of MAPKs in mTORC1 activation.

(B) p38δ was required for p62 phosphorylation at T269/S272 in response to amino acids. p38δ-deficient HEK293T cells generated with the CRISPR/CAS9 system. Cells were deprived of amino acids for 50 min and then stimulated with amino acids for 15 min. Cell lysates were immunoblotted for the indicated proteins.

(C) RagB^{GTP} overexpression rescued amino-acid-induced mTOR activation in p38δ-deficient cells. Control and p38δ-deficient HEK293T cells, expressing FLAG-RagB^{GTP}, were treated as in (B). Cell lysates were immunoblotted for the indicated proteins.

(D) p38δ was not required for insulin-induced mTORC1 activation. Control and p38δ-deficient HEK293T cells were deprived of serum for 24 hr and then stimulated with insulin for the indicated durations. Cell lysates were immunoblotted to detect the indicated proteins.

(E) p38δ overexpression promotes p62 phosphorylation at T269/S272. HEK293T cells were transfected with the indicated plasmids and immunoblotted for the specified proteins.

(F) p38δ kinase activity was required for p62 phosphorylation. HEK293T cells were transfected with the indicated plasmids and immunoblotted for the specified proteins.

(G) p38δ directly phosphorylated p62 at T269/S272 in vitro. An in vitro phosphorylation assay using recombinant p62 and recombinant p38δ is shown.

(H) T269/S272 sites accounted for p62 phosphorylation by p38δ. FLAG-tagged immunoprecipitates from HEK293T cells were phosphorylated in vitro by recombinant p38δ with ATPγS, followed by PNBM alkylation and immunoblotting for the indicated proteins.

(I) p38δ kinase activity was activated by amino acids. HEK293T cells transfected with the indicated plasmids were treated as in (B). In vitro phosphorylation was carried out with the FLAG-tagged immunoprecipitates and MBP-p62 recombinant protein as a substrate.

(J) MEKK3 was required for p38δ-induced p62 phosphorylation by amino acids. shNT or shMEKK3 HEK293T cells transfected with the indicated plasmids were treated as in (B). In vitro phosphorylation was carried out with the FLAG-tagged immunoprecipitates, and MBP-p62 recombinant protein was used as the substrate.

(K) MEK3/6 was required for p62 phosphorylation and mTORC1 activation in response to amino acids. HEK293T cells transfected with scramble siRNA or MEK3 and MEK6 siRNAs and FLAG-RagB^{GTP} were treated as in (B). Cell lysates were immunoblotted for the indicated proteins.

(legend continued on next page)

recombinant p62 was incubated with active recombinant MEKK3 in an in vitro kinase assay, we found that MEKK3 was not able to directly phosphorylate p62 (Figure S3A). These results strongly suggest the existence of other kinase that acts downstream of MEKK3 to phosphorylate p62 in response to amino acids. Our previously published data showed that CDK1 was able to phosphorylate p62 at residues T269/S272 during mitosis (Linares et al., 2011). However, a selective CDK1 inhibitor did not affect p62 phosphorylation in response to amino acids (Figure S3B). To identify that kinase, because MEKK3 is a MAP3K, we reasoned that a MAP2K/MAPK cascade could act downstream of MEKK3 to phosphorylate p62. To address this possibility, we individually knocked down all the members of the five distinct groups of MAPKs characterized in mammals (Figure 3A). Cells were stimulated with amino acids, as above, and the activation of mTORC1 was determined. Notably, only depletion of p38δ (MAPK13) severely impaired amino-acid-induced activation of mTORC1 (Figures 3A and S3C). Importantly, knockout of p38δ by CRISPR/Cas9 severely abolished p62 phosphorylation and mTORC1 activation in cells stimulated with amino acids, which was rescued by the expression of active RagB (Figures 3B and 3C). Of note, p38δ-deficient cells displayed normal insulin-induced mTORC1 activation (Figure 3D). Similar results were obtained with two other independent CRISPR/Cas9-generated p38δ KO clones (Figure S3D). Furthermore, the pharmacological inhibition of p38δ severely abrogated mTORC1 activation and p62 phosphorylation by amino acids (Figure S3E). Interestingly, we also found that the overexpression of WT, but not of a kinase-inactive p38δ (T180A/Y182F) mutant, was able to induce the phosphorylation of $p62^{WT}$, but not of $p62^{T269/S272AA}$ (Figures 3E and 3F). Taken together, these results demonstrate that p38δ is responsible for p62 phosphorylation and mTORC1 activation by amino acids. To determine whether p62 is actually a direct substrate of p38δ, we incubated bacterially expressed recombinant p62 with active p38δ in an in vitro kinase assay and found that p38δ directly phosphorylated p62 at T269/S272 (Figure 3G). To confirm that these residues account for p62 phosphorylation by p38δ, purified $p62^{WT}$ and $p62^{T269/S272AA}$ were phosphorylated in vitro with ATP-γ-S and recombinant active p38δ. Figure 3H demonstrates that p62 phosphorylation by p38δ was completely abolished in the $p62^{T269/S272AA}$ mutant, as compared to $p62^{WT}$, indicating that p38δ is a bona fide direct p62 T269/S272 kinase that channels MEKK3 signals in amino-acid-activated cells.

If this model is correct, then p38δ should be activated by amino acids in a MEKK3-dependent manner. To determine whether this was the case, HEK293T cells were transfected with FLAG-tagged p38δ, after which cells were treated with amino acids at different times as described above. Transfected p38δ was immunoprecipitated with an anti-FLAG antibody, and its ability to phosphorylate recombinant p62 was determined in an in vitro kinase assay. Interestingly, p38δ from shNT cells that were stimulated with amino acids displayed higher enzymatic activity toward recombinant p62 than p38δ from unstimulated shNT cells (Figure 3I). The finding that amino acid stimulation did not increase the activity of p38δ in shMEKK3 cells (Figure 3J) clearly established that p38δ is a critical downstream target of MEKK3 in the nutrient-sensing cascade that activates mTORC1 through p62 phosphorylation. To identify the kinase that links MEKK3 to p38δ, we tested whether MEK3 and MEK6 might be the MAP2Ks upstream of p38δ. Notably, the simultaneous depletion of MEK3 and MEK6 severely impaired amino-acid-induced mTORC1 activation and p62 phosphorylation, which was rescued by the expression of active RagB (Figure 3K). Furthermore, the kinase activity of MEK3 was stimulated in amino-acid-treated cells (Figure 3L). Collectively, these results demonstrate that MEKK3 is the apical kinase in an amino-acid-sensing cascade that includes MEK3/MEK6 and p38δ and that leads to p62 phosphorylation, which is a critical step for mTORC1 activation in response to amino acids (Figure 3M).

MEKK3 and p38δ Control Lysosomal Translocation of mTOR

To be activated by amino acid stimulation, mTORC1 must undergo translocation from the cytoplasm to the lysosome (Sancak et al., 2008). Given that MEKK3 and p38δ are necessary for amino-acid-induced mTORC1 activity, we next investigated the subcellular localization of MEKK3 and p38δ by confocal immunofluorescence microscopy in both starved and amino-acid-stimulated cells. Double staining of endogenous MEKK3 or p38δ and lysosomal-associated membrane protein 2 (LAMP2) revealed the localization of both kinases at the lysosome, which was independent of nutrient availability (Figures 4A and 4B). The antibodies used in this experiment were validated for immunofluorescence in MEKK3 or p38δ knocked down cells (Figure S4). Cell fractionation confirmed the constitutive localization of MEKK3, p38δ, and p62, along with Lamp2, in the heavy membrane lysosomal fraction (Figure 4C). Of great functional relevance, the knockdown of either MEKK3 or p38δ impaired the colocalization of mTORC1 with LAMP2 in response to amino acids (Figure 4D), demonstrating that p38δ and MEKK3, like p62, are required for mTORC1 translocation to the lysosome.

Role of the MEKK3/p38δ Cascade in the Polyubiquitination of mTOR

TRAF6 is recruited to the p62-mTORC1 complex upon amino acid stimulation, and this promoted the K63 polyubiquitination of mTOR, a key event in amino-acid-dependent activation of mTORC1 (Linares et al., 2013). Our current results link this process to the MEKK3/p38δ cascade, because depletion of either kinase severely impaired the interaction of TRAF6 with p62 (Figures 5A and 5B). This suggests a critical role for the phosphorylation of p62 by the MEKK3/p38δ cascade in the binding of TRAF6 to p62, consistent with the fact that $p62^{T269/S272AA}$ did

(L) MEK3 is activated in response to amino acids. HEK293T cells transfected with the indicated plasmids were treated as in (B). FLAG-tagged MEK3 immunoprecipitates were used in an in vitro phosphorylation, using MyBP as substrate, with ATPγS followed by PNBM alkylation and immunoblotting for the indicated proteins.

(M) Schematic showing that MEK3/6-p38δ channels MEKK3-induced phosphorylation of p62 and mTORC1 activation by amino acids.

Results are representative of three experiments. See also Figure S3.

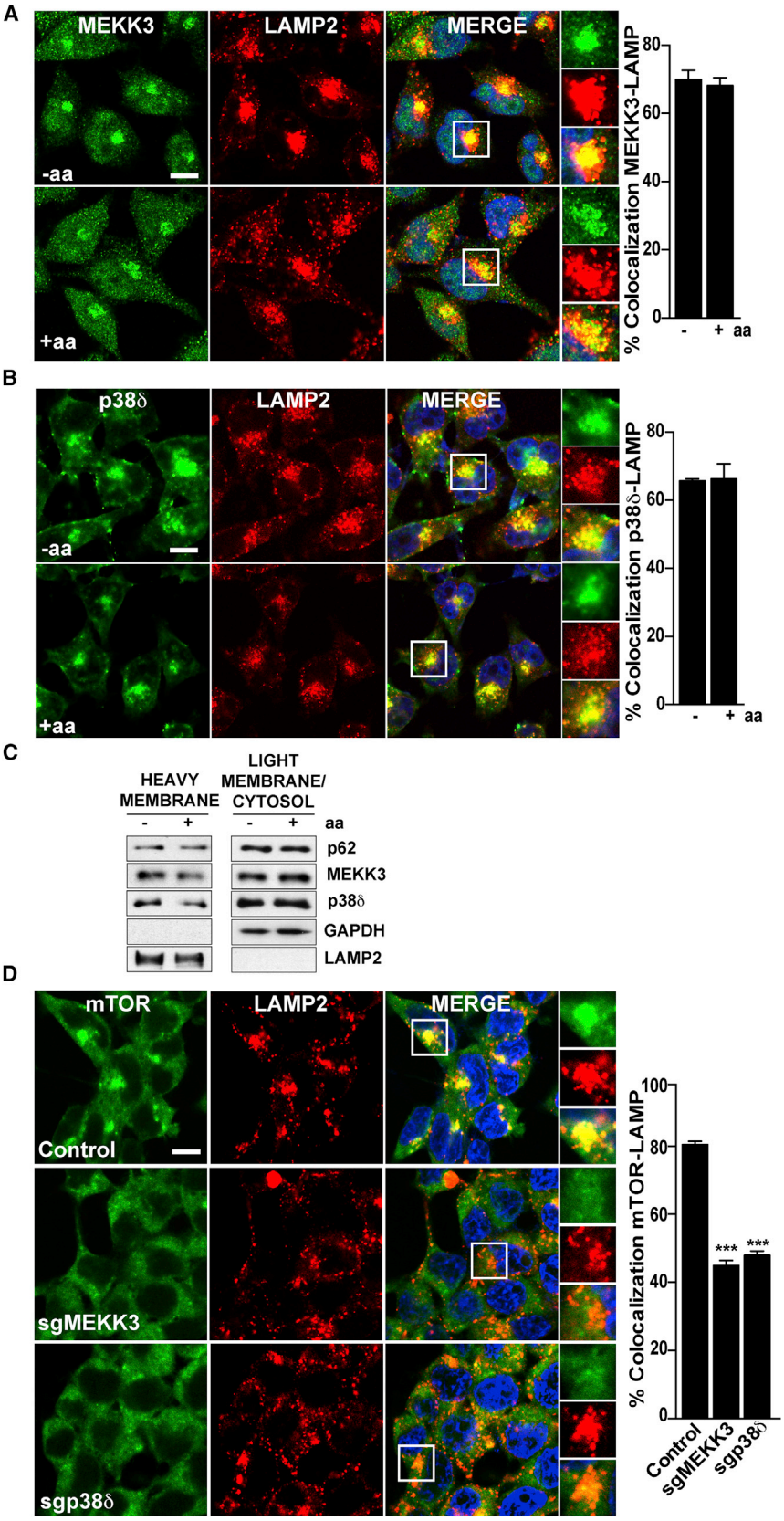

Figure 4. MEKK3/p38δ Cascade Is Required for the Lysosomal Translocation of mTOR

(A and B) MEKK3 and p38δ localize at the lysosome in an amino-acid-independent manner. Images of HeLA cells co-immunostained for MEKK3 and LAMP2 (A) or p38δ and LAMP2 (B) are shown. Cells were starved for 50 min and then stimulated with amino acids for 10 min before processing. In all images, graphs show the areas of staining overlap (merge). The scale bars represent 10 μm. The quantification of colocalization was carried out on at least 15 cells per condition from two independent experiments. Results are shown as means ± SEM.

(C) MEKK3, p38δ, and p62 were present in the lysosomal fraction. HEK293T cells were treated as in (A), and lysates were separated into heavy membrane and light/cytosolic fractions.

(D) MEKK3 and p38δ deficiency prevented amino-acid-induced translocation of mTOR to lysosomes. Images of control, MEKK3-deficient, or p38δ-deficient HEK293T cells treated and analyzed as in (A) that were co-immunostained to detect mTOR and LAMP2 are shown. The scale bars represent 10 μm. Results are shown as means ± SEM. ***$p < 0.001$. Images are representative of two independent experiments. See also Figure S4.

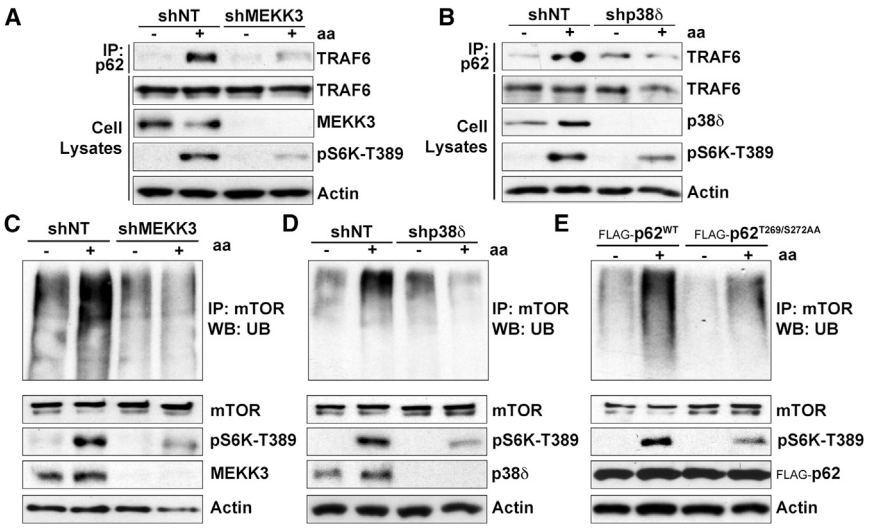

Figure 5. The MEKK3/p38δ Cascade Was Required for TRAF6-Catalyzed K63 Polyubiquitination of mTOR in Response to Amino Acids

(A and B) Knockdown of MEKK3 or p38δ impaired the interaction of TRAF6 with p62 in response to amino acids. shNT, shMEKK3, or shp38δ HEK293T cells were deprived of amino acids for 50 min and then restimulated with amino acids for 30 min. Cell lysates and p62 immunoprecipitates were analyzed by western blot for the indicated proteins.

(C–E) MEKK3, p38δ, and p62 phosphorylation were required for polyubiquitination of mTOR in response to amino acids. shNT, shMEKK3, and shp38δ HEK293T cells or cells stably expressing FLAG-p62^{WT} or FLAG-p62$^{T269/S272AA}$ were treated as in (A). Cell lysates and mTOR immunoprecipitates were immunoblotted for the indicated proteins.

Results are representative of three experiments.

not interact with TRAF6 in amino-acid-stimulated cells (Figure 1I). As predicted by this model, endogenous polyubiquitination of mTOR in response to amino acids was severely inhibited by the deficiency of either MEKK3 or p38δ (Figures 5C and 5D). Furthermore, the endogenous polyubiquitination of mTOR in response to amino acids was inhibited in cells expressing the p62$^{T269/S272AA}$ mutant compared with those expressing p62^{WT} (Figure 5E). Collectively, these data demonstrate that p62 phosphorylation by p38δ is a key event in the recruitment of mTORC1 to the lysosome and in its subsequent activation by TRAF6-mediated polyubiquitination.

The MEKK3/p38δ Cascade Contributes to Cell Proliferation and Autophagy

A well-established function of mTORC1 is to control cell size (Fingar et al., 2002). In keeping with a critical role for MEKK3 and p38δ in the activation of mTORC1, cells deficient in MEKK3, p38δ, or p62 were significantly smaller than WT controls (Figure 6A). On the other hand, it is known that mTORC1 activation promotes cell proliferation and transformation while inhibiting autophagy (Kim et al., 2011; Yu et al., 2010). Consistent with this, the knockdown of MEKK3 or p38δ in PC3 prostate cancer (PCa) cells significantly reduced cell proliferation under normal growing conditions (Figures 6B and 6C), and this effect was rescued by the expression of a constitutively active mutant of RagB (Figures 6D and 6E). Given that nutrient starvation induces autophagy through inhibition of mTORC1 (Kim et al., 2011; Yu et al., 2010), we knocked down MEKK3 or p38δ and determined the effect on autophagy. Interestingly, reduction in the levels of either of these kinases resulted in enhanced LC3 processing, which was even more apparent when cells were incubated with bafilomycin A1, an inhibitor of autophagosomal and lysosomal fusion (Figures 6F–6I). We also analyzed autophagic flux using the reporter GFP-mCherry-LC3 (Kimura et al., 2007), which allows the identification of autolysosomes (mCherry-positive/GFP-negative; red dots) and autophagosomes (mCherry-positive/GFP-positive; yellow dots). Our data showed that the total numbers of autophagosomes and autolysosomes under basal and amino acid starvation conditions were higher in the MEKK3- and p38δ-deficient cells (Figures 6J and 6K). Taken together, these results demonstrate that the MEKK3/p38δ cascade modulates autophagy in response to nutrient starvation, consistent with its role in the regulation of mTORC1 activation.

Relevance of the MEKK3/p38δ/p62/mTOR Axis in Prostate Cancer

To investigate the relevance of the p62/MEKK3/p38δ cascade in the activation of mTOR in PCa, we profited from a recently developed technology for creating 3D prostate organoid cultures (Gao et al., 2014; Karthaus et al., 2014). Murine prostate organoids faithfully recapitulate the in vivo phenotypes of genetic PCa mouse models and can be easily manipulated (Gao et al., 2014; Karthaus et al., 2014). Thus, we isolated prostate epithelial cells from PTEN-deficient mice and subjected them to lentiviral infection to selectively knock down MEKK3, p38δ, or p62 and then cultured them in 3D organoid conditions. Interestingly, we found that the inactivation of MEKK3, p38δ, or p62 decreased the efficiency of organoid formation and size of organoids and reverted the hyperplastic phenotype of the PTEN$^{-/-}$ organoids (Figures 7A and 7B). This strongly suggests an important role for the MEKK3/p38δ cascade in PCa. Notably, the deficiency in p62, MEKK3, or p38δ in these organoids resulted in severe impairment of S6K and 4EBP1 phosphorylation in this model (Figure 7C). Consistent with these observations, immunohistochemical analysis of prostates from PTEN$^{+/-}$ mice showed increased expression of MEKK3, p38δ, and p62, as well as the activation of S6 phosphorylation, which was used as a surrogate marker of mTORC1 activity, in PIN areas of the prostate, as compared to normal glands (Figure 7D). Furthermore, we used double immunofluorescence to analyze the colocalization of p38δ either with p62 or with pS6 in sections of human PCa and normal prostate tissue. Of great interest, we found that p62 and p38δ levels were increased and colocalized with enhanced

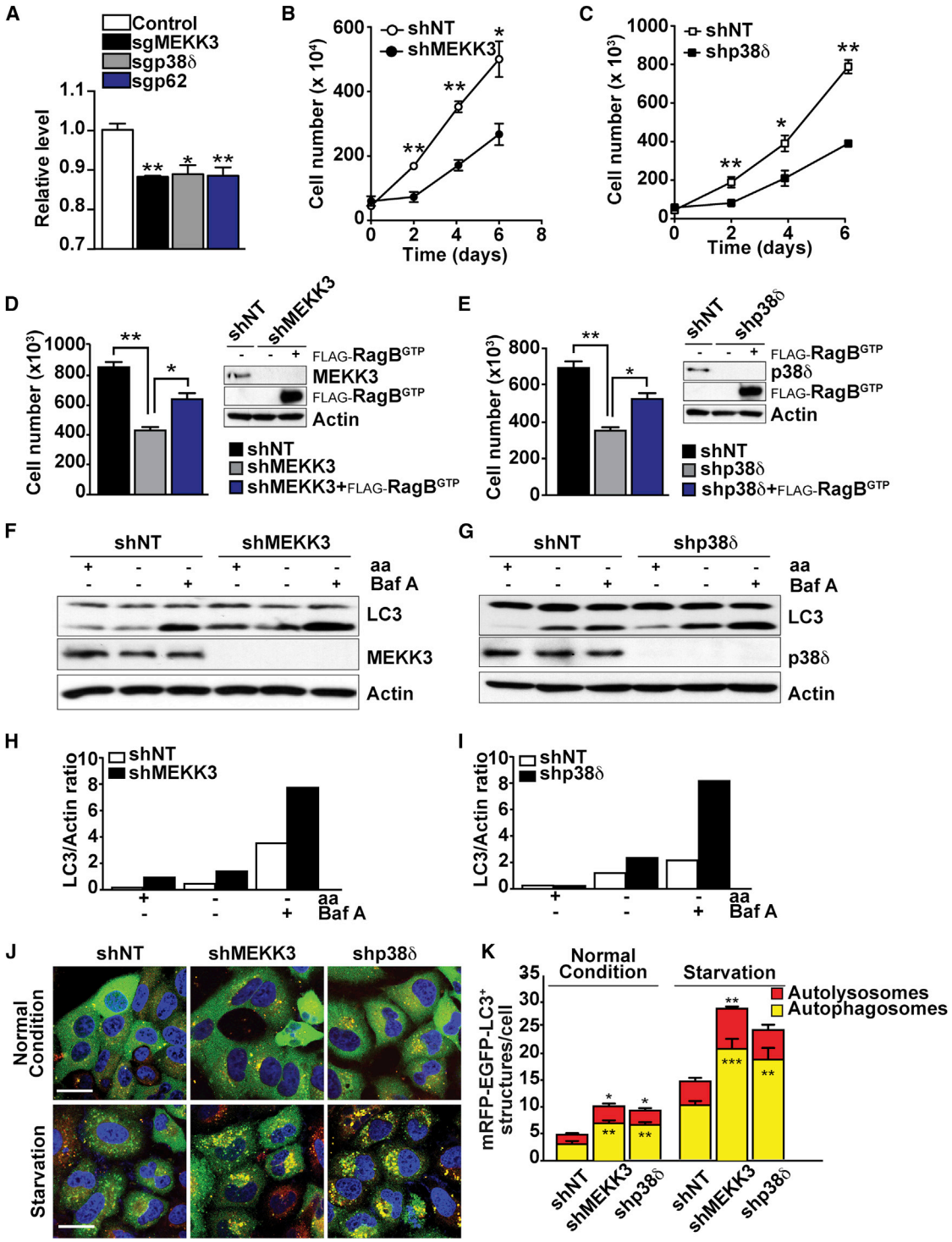

Figure 6. The MEKK3/p38δ Cascade Controlled Cell Proliferation and Autophagy through mTORC1 Activation

(A) MEKK3, p62, or p38δ deficiencies reduced cell size. Results are shown as means ± SEM (n = 3). *p < 0.05; **p < 0.01.

(B and C) Knockdown of MEKK3 or p38δ reduced cell proliferation under normal growing conditions. shNT, shMEKK3, or shp38δ PC3 cells were cultured under normal growing conditions, and cell viability was determined by trypan blue exclusion assay. Results are shown as means ± SEM (n = 3). *p < 0.05; **p < 0.01.

(D and E) RagB^{GTP} overexpression rescued the defects in cell proliferation in MEKK3- or p38δ-knockdown cells. PC3 cells stably expressing FLAG-RagB^{GTP} were infected with shNT, shMEKK3, or shp38δ lentiviral vectors. Cell lysates were analyzed by western blot, and cell viability was determined as in (C). Results are shown as means ± SEM (n = 3). *p < 0.05; **p < 0.01.

(legend continued on next page)

pS6 staining, in tumor tissues as compared to normal controls (Figure 7E). We next analyzed the expression of MEKK3, p38δ, p62, and phospho-S6 in PCa tissue microarrays by immunohistochemistry. Interestingly, our data showed much stronger expression of all these proteins in aggressive tumors with high Gleason score (GS 7–10) than in those with low Gleason score (GS 2–6; Figure 7F). Importantly, MEKK3 and p38δ expression significantly correlated with p62 and phospho-S6 in these human PCa samples (Figure 7G). Taken together, these results established that the PB1-driven MEKK3/p38δ/p62/mTOR pathway is relevant to PCa.

DISCUSSION

The mechanisms whereby cells couple nutrient availability to anabolism and cell growth are being progressively unveiled, and the role of mTORC1 in these processes is well established (Jewell and Guan, 2013; Laplante and Sabatini, 2012; Shimobayashi and Hall, 2014). A major breakthrough in the field was the identification of the lysosome as a critical organelle where mTORC1 is recruited via the Rag proteins and then activated by as-yet-undefined mechanisms. In addition, how mTORC1 senses the availability of nutrients, and specifically of amino acids, is a fundamental problem in the field that needs to be resolved. Here, we show that the signaling adaptor p62, which we previously demonstrated to contribute to mTORC1 activation by amino acids (Duran et al., 2011), is phosphorylated at two specific residues by p38δ through a MEKK3/MEK3/6-driven cascade that enables the recruitment of TRAF6 to the lysosome. This creates a signaling scaffold with the core mTORC1 complex that results in the K63 polyubiquitination of mTOR and its activation in response to amino acids but independent of insulin. Therefore, p62 emerges as a platform that facilitates the recruitment and efficient activation of mTORC1. Interestingly, the specificity of this process is provided by the selective interaction of MEKK3 with p62 through their respective PB1 domains. In this regard, although different MAPKs have previously been implicated in the negative or positive control of mTORC1, primarily in response to stress stimuli (Cully et al., 2010; Li et al., 2003; Wu et al., 2011; Zheng et al., 2011), our data reveal a specific role for p38δ in mTOR activation in the nutrient cascade as part of a PB1-directed complex. Our studies contribute to a better understanding of the activation of mTORC1 by amino acids, but also they provide context for previously reported p62 phosphorylation events. That is, recent data demonstrate that p62 is phosphorylated at S351, which serves to increase its binding affinity for Keap1 and competitively inhibits the Keap1-Nrf2 interaction (Ichimura et al., 2013). This results in the stabilization of Nrf2 and the subsequent expression of genes encoding antioxidant proteins and anti-inflammatory enzymes (Ichimura et al., 2013). Interestingly, at least one of the kinases that can target p62's S351 is mTOR itself. Therefore, it is tempting to speculate that the MEKK3-directed phosphorylation of p62 at T269/S272 serves to activate mTORC1, which then phosphorylates p62's S351 to activate Nrf2 to protect cells from oxidative stress. In cancer, this could be highly relevant because tumor cells need to remove excess ROS while maintaining high levels of proliferation. Therefore, our model predicts that p62 is a crucial regulator of cancer cell proliferation by influencing cell growth through mTORC1 and cell survival through an mTORC1-p62-driven anti-oxidative mechanism.

Interestingly, we have recently reported that MEKK3 is part of another PB1 complex that activates a canonical MEK4/JNK cascade to regulate inflammation in macrophages in response to lipids, another type of nutrients that can trigger an inflammatory response when present in excess (Hernandez et al., 2014). This distinct MEKK3 pathway is orchestrated by the interaction of MEKK3 with NBR1 through their respective PB1 domains (Hernandez et al., 2014). Therefore, two PB1 scaffolds, p62 in mTORC1 and NBR1 in inflammation, use MEKK3 to deliver their respective signals in response to different nutrients. How the interaction of MEKK3 with either p62 or NBR1 orchestrates the p38δ or the JNK pathways, respectively, is not clear and will likely need more-detailed structural studies to be fully understood.

In summary, the work presented here describes a nutrient-sensing pathway that is selectively activated in response to amino acids and is also operative in cancer cells. This kinase cascade is organized by a platform that depends on p62 PB1-domain interactions and is highly upregulated during cancer progression. Different components of the cascade are overexpressed in PCa in a manner that is correlated with tumor stage, which suggests that the cascade is essential for tumor development. Because kinases are eminently druggable targets, our findings have the potential to open new avenues for designing novel treatments for cancer.

EXPERIMENTAL PROCEDURES

Mice

$PTEN^{+/-}$ and $PTEN^{fl/fl}$-PBcre mice were described previously (Fernandez-Marcos et al., 2009). Both mouse strains were generated in a C57BL/6 background. All mice were born and maintained under pathogen-free conditions. Animal handling and experimental procedures conformed to institutional guidelines (Sanford-Burnham Medical Research Institute Institutional Animal Care and Use Committee).

Generation of Knockout Cell Lines

To knock out genes in cell lines, guide RNAs targeting MEKK3, p38δ, and p62 were designed using the CRISPR design tool at http://crispr.mit.edu/ and cloned into a bicistronic expression vector (PX458) containing human-codon-optimized Cas9 fused to EGFP through T2A sequence and the RNA

(F–I) Knockdown of MEKK3 or p38δ promoted autophagy in response to nutrient deprivation. shNT, shMEKK3, or shp38δ PC3 cells were deprived of amino acids and serum for 4 hr in the absence or presence of bafilomycin A1. Cell lysates were immunoblotted for the indicated proteins. Graphs represent LC3-II/actin ratio as measured by densitometry.

(J and K) Knockdown of MEKK3 or p38δ promoted increased autophagic flux. Images of shNT, shMEKK3, or shp38δ cells stably expressing GFP-mCherry-LC3 and treated as in (G) are shown. The scale bars represent 10 μm. Quantification of the number of autophagosomes and autolysosomes per cell is shown. Results are shown as means ± SEM (n = 20). *p < 0.05; **p < 0.01; ***p < 0.001.

Results are representative of three experiments.

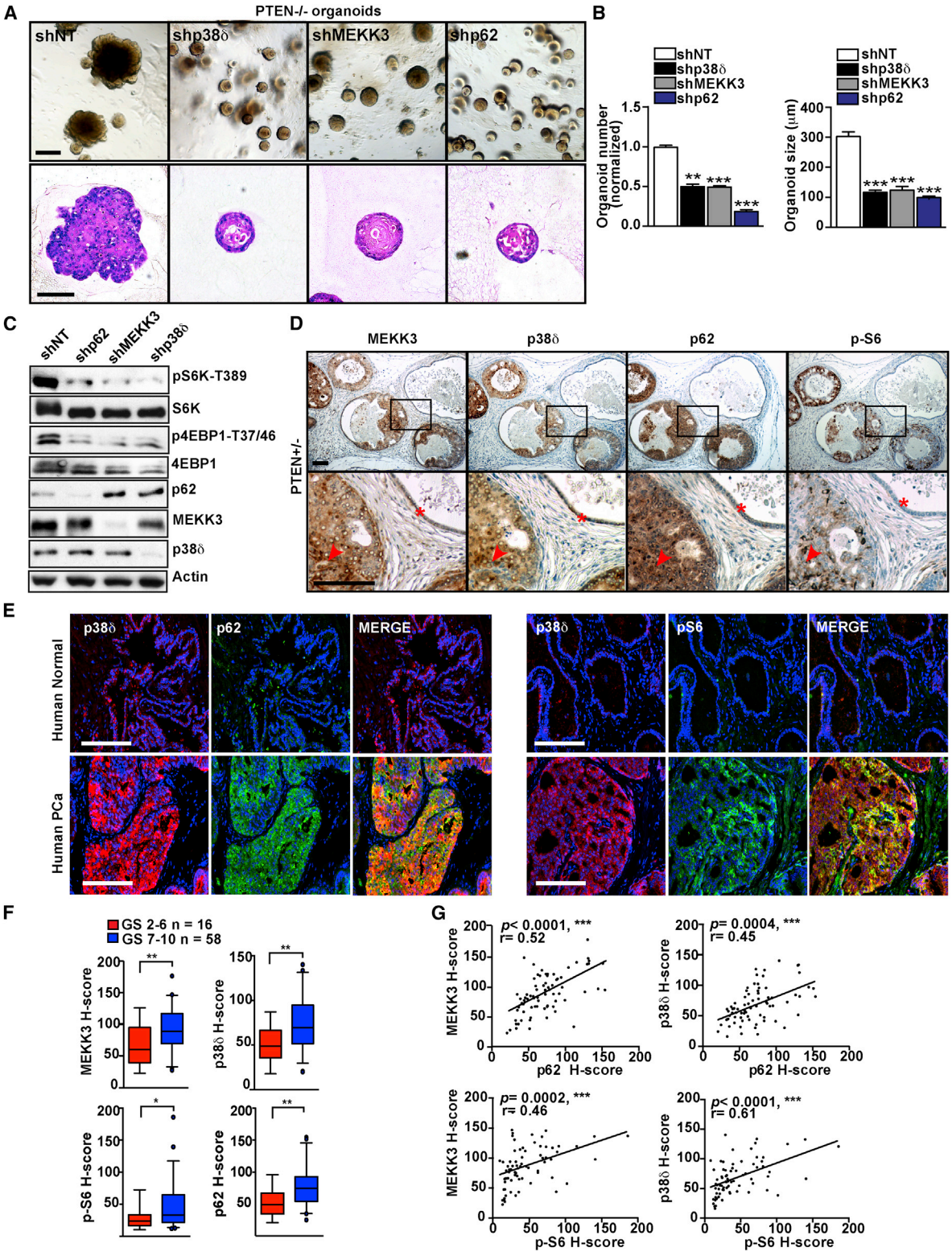

Figure 7. MEKK3/p38δ/p62/mTOR Is Relevant to Prostate Cancer

(A) Knockdown of MEKK3, p38δ, or p62 led to a reduction in the efficiency of organoid formation, size, and hyperplastic phenotype of PTEN-null prostate organoids. Representative images of organoids and H&E staining are shown. Prostate organoids were prepared from PTEN$^{fl/fl}$-PBcre mice and infected with lentiviral vectors for shNT, shp62, shMEKK3, and shp38δ. Organoids were analyzed after 7 days in culture. The scale bars represent 100 μm.

(legend continued on next page)

components (Addgene). Additional detailed procedures are described in the Supplemental Experimental Procedures.

Statistical Analysis

All the statistical tests are justified for every figure. Data are presented as the mean ± SEM. Significant differences between groups were determined using a Student's t test (two-tailed unpaired) when the data met the normal distribution tested by D'Agostino test. If the data did not meet this test, a Mann-Whitney test was used. The significance level for statistical testing was set at $p < 0.05$. All experiments were performed at least two or three times.

SUPPLEMENTAL INFORMATION

Supplemental Information includes Supplemental Experimental Procedures and four figures and can be found with this article online at http://dx.doi.org/10.1016/j.celrep.2015.07.045.

AUTHOR CONTRIBUTIONS

J.F.L. performed most of experiments of this study. A.D. contributed the prostate organoid experiments and IHC staining. M.R.-C. generated CRISPR/CAS9 clones. P.A.-B. contributed to the siRNA screening. A.C. performed the proteomic analysis. M.T.D.-M. and J.M. conceived and supervised the project. M.T.D.-M., J.F.L., and J.M. wrote the manuscript with assistance from all the authors.

ACKNOWLEDGMENTS

NIH grants R01CA132847 (to J.M.), R01CA172025 (to J.M.), R01CA192642 (to M.T.D.-M.), and 5P30CA030199 (to M.T.D.-M. and J.M.) funded this work. Additional support was provided by DoD grants W81XWH-13-1-0353 (to M.T.D-M.) and W81XWH-13-1-0354 (to J.M.). We thank Maryellen Daston for editing this manuscript, Diantha LaVine for the artwork, and Wei Liu and the personnel of the Cell Imaging, Animal Facility, Histology, Functional Genomics, Proteomics, and Viral Vectors Shared Resources at SBMRI for technical assistance.

Received: June 12, 2015
Revised: July 8, 2015
Accepted: July 23, 2015
Published: August 13, 2015

REFERENCES

Bar-Peled, L., Chantranupong, L., Cherniack, A.D., Chen, W.W., Ottina, K.A., Grabiner, B.C., Spear, E.D., Carter, S.L., Meyerson, M., and Sabatini, D.M. (2013). A Tumor suppressor complex with GAP activity for the Rag GTPases that signal amino acid sufficiency to mTORC1. Science *340*, 1100–1106.

Budanov, A.V., and Karin, M. (2008). p53 target genes sestrin1 and sestrin2 connect genotoxic stress and mTOR signaling. Cell *134*, 451–460.

Chantranupong, L., Wolfson, R.L., Orozco, J.M., Saxton, R.A., Scaria, S.M., Bar-Peled, L., Spooner, E., Isasa, M., Gygi, S.P., and Sabatini, D.M. (2014). The Sestrins interact with GATOR2 to negatively regulate the amino-acid-sensing pathway upstream of mTORC1. Cell Rep. *9*, 1–8.

Cully, M., Genevet, A., Warne, P., Treins, C., Liu, T., Bastien, J., Baum, B., Tapon, N., Leevers, S.J., and Downward, J. (2010). A role for p38 stress-activated protein kinase in regulation of cell growth via TORC1. Mol. Cell. Biol. *30*, 481–495.

Durán, R.V., and Hall, M.N. (2012). Regulation of TOR by small GTPases. EMBO Rep. *13*, 121–128.

Duran, A., Linares, J.F., Galvez, A.S., Wikenheiser, K., Flores, J.M., Diaz-Meco, M.T., and Moscat, J. (2008). The signaling adaptor p62 is an important NF-kappaB mediator in tumorigenesis. Cancer Cell *13*, 343–354.

Duran, A., Amanchy, R., Linares, J.F., Joshi, J., Abu-Baker, S., Porollo, A., Hansen, M., Moscat, J., and Diaz-Meco, M.T. (2011). p62 is a key regulator of nutrient sensing in the mTORC1 pathway. Mol. Cell *44*, 134–146.

Efeyan, A., Schweitzer, L.D., Bilate, A.M., Chang, S., Kirak, O., Lamming, D.W., and Sabatini, D.M. (2014). RagA, but not RagB, is essential for embryonic development and adult mice. Dev. Cell *29*, 321–329.

Fernandez-Marcos, P.J., Abu-Baker, S., Joshi, J., Galvez, A., Castilla, E.A., Cañamero, M., Collado, M., Saez, C., Moreno-Bueno, G., Palacios, J., et al. (2009). Simultaneous inactivation of Par-4 and PTEN in vivo leads to synergistic NF-kappaB activation and invasive prostate carcinoma. Proc. Natl. Acad. Sci. USA *106*, 12962–12967.

Fingar, D.C., Salama, S., Tsou, C., Harlow, E., and Blenis, J. (2002). Mammalian cell size is controlled by mTOR and its downstream targets S6K1 and 4EBP1/eIF4E. Genes Dev. *16*, 1472–1487.

Gao, D., Vela, I., Sboner, A., Iaquinta, P.J., Karthaus, W.R., Gopalan, A., Dowling, C., Wanjala, J.N., Undvall, E.A., Arora, V.K., et al. (2014). Organoid cultures derived from patients with advanced prostate cancer. Cell *159*, 176–187.

Groenewoud, M.J., Goorden, S.M., Kassies, J., Pellis-van Berkel, W., Lamb, R.F., Elgersma, Y., and Zwartkruis, F.J. (2013). Mammalian target of rapamycin complex I (mTORC1) activity in ras homologue enriched in brain (Rheb)-deficient mouse embryonic fibroblasts. PLoS ONE *8*, e81649.

Guertin, D.A., and Sabatini, D.M. (2007). Defining the role of mTOR in cancer. Cancer Cell *12*, 9–22.

Hay, N., and Sonenberg, N. (2004). Upstream and downstream of mTOR. Genes Dev. *18*, 1926–1945.

Hernandez, E.D., Lee, S.J., Kim, J.Y., Duran, A., Linares, J.F., Yajima, T., Müller, T.D., Tschöp, M.H., Smith, S.R., Diaz-Meco, M.T., and Moscat, J. (2014). A macrophage NBR1-MEKK3 complex triggers JNK-mediated adipose tissue inflammation in obesity. Cell Metab. *20*, 499–511.

Ichimura, Y., Waguri, S., Sou, Y.S., Kageyama, S., Hasegawa, J., Ishimura, R., Saito, T., Yang, Y., Kouno, T., Fukutomi, T., et al. (2013). Phosphorylation of p62 activates the Keap1-Nrf2 pathway during selective autophagy. Mol. Cell *51*, 618–631.

(B) Quantification of the efficiency of organoid formation and size in the experiment shown in (A). The scale bars represent 100 μm. Results are presented as mean ± SEM. *$p < 0.05$; **$p < 0.01$; ***$p < 0.001$.

(C) Knockdown of MEKK3, p38δ, or p62 in PTEN-null prostate organoids led to decreased mTORC1 activation. Cell lysates from (A) were immunoblotted for the indicated proteins.

(D) Increased expression of MEKK3, p38δ, p62, and S6 phosphorylation in PIN areas (red arrows) of $PTEN^{+/-}$ prostates, compared with normal prostate glands (asterisks). Representative images of MEKK3, p38δ, p62, and phospho-S6 staining of primary PCa samples from $PTEN^{+/-}$ mice are shown. The scale bars represent 25 μm.

(E) Human prostate shows increased expression of p38δ, p62, and S6 phosphorylation in tumor tissue, as compared with normal tissue. Images of human prostate co-immunostained for p38δ and p62 or and p38δ and p-S6 are shown. The scale bars represent 100 μm.

(F) Increased expression of MEKK3, p38δ, p62, and S6 phosphorylation in human prostate tissue microarray (TMA). Box plot graphs show a statistical analysis of MEKK3 ($p = 0.006$), p38δ ($p = 0.004$), p62 ($p = 0.003$), or phospho-S6 ($p = 0.049$) expression in prostate tumors with GS 7–10 compared to prostate tissue with GS 2–6. Results are presented as mean ± SEM. *$p < 0.05$; **$p < 0.01$.

(G) MEKK3 and p38δ expression in human prostate tumors was correlated with p62 and phospho-S6. Correlation plots show the relationship between MEKK3/p62, MEKK3/phosho-S6, p38δ/p62, and p38δ/phospho-S6 (a.u.). The coefficient of correlation (r) and the p value (p) are indicated.

Jewell, J.L., and Guan, K.L. (2013). Nutrient signaling to mTOR and cell growth. Trends Biochem. Sci. *38*, 233–242.

Jewell, J.L., Kim, Y.C., Russell, R.C., Yu, F.X., Park, H.W., Plouffe, S.W., Tagliabracci, V.S., and Guan, K.L. (2015). Metabolism. Differential regulation of mTORC1 by leucine and glutamine. Science *347*, 194–198.

Karthaus, W.R., Iaquinta, P.J., Drost, J., Gracanin, A., van Boxtel, R., Wongvipat, J., Dowling, C.M., Gao, D., Begthel, H., Sachs, N., et al. (2014). Identification of multipotent luminal progenitor cells in human prostate organoid cultures. Cell *159*, 163–175.

Kim, J., Kundu, M., Viollet, B., and Guan, K.L. (2011). AMPK and mTOR regulate autophagy through direct phosphorylation of Ulk1. Nat. Cell Biol. *13*, 132–141.

Kimura, S., Noda, T., and Yoshimori, T. (2007). Dissection of the autophagosome maturation process by a novel reporter protein, tandem fluorescent-tagged LC3. Autophagy *3*, 452–460.

Laplante, M., and Sabatini, D.M. (2012). mTOR signaling in growth control and disease. Cell *149*, 274–293.

Li, Y., Inoki, K., Vacratsis, P., and Guan, K.L. (2003). The p38 and MK2 kinase cascade phosphorylates tuberin, the tuberous sclerosis 2 gene product, and enhances its interaction with 14-3-3. J. Biol. Chem. *278*, 13663–13671.

Linares, J.F., Amanchy, R., Greis, K., Diaz-Meco, M.T., and Moscat, J. (2011). Phosphorylation of p62 by cdk1 controls the timely transit of cells through mitosis and tumor cell proliferation. Mol. Cell. Biol. *31*, 105–117.

Linares, J.F., Duran, A., Yajima, T., Pasparakis, M., Moscat, J., and Diaz-Meco, M.T. (2013). K63 polyubiquitination and activation of mTOR by the p62-TRAF6 complex in nutrient-activated cells. Mol. Cell *51*, 283–296.

Matsumoto, G., Wada, K., Okuno, M., Kurosawa, M., and Nukina, N. (2011). Serine 403 phosphorylation of p62/SQSTM1 regulates selective autophagic clearance of ubiquitinated proteins. Mol. Cell *44*, 279–289.

Moscat, J., and Diaz-Meco, M.T. (2009). p62 at the crossroads of autophagy, apoptosis, and cancer. Cell *137*, 1001–1004.

Moscat, J., and Diaz-Meco, M.T. (2011). Feedback on fat: p62-mTORC1-autophagy connections. Cell *147*, 724–727.

Moscat, J., Diaz-Meco, M.T., Albert, A., and Campuzano, S. (2006). Cell signaling and function organized by PB1 domain interactions. Mol. Cell *23*, 631–640.

Nakamura, K., Kimple, A.J., Siderovski, D.P., and Johnson, G.L. (2010). PB1 domain interaction of p62/sequestosome 1 and MEKK3 regulates NF-kappaB activation. J. Biol. Chem. *285*, 2077–2089.

Petit, C.S., Roczniak-Ferguson, A., and Ferguson, S.M. (2013). Recruitment of folliculin to lysosomes supports the amino acid-dependent activation of Rag GTPases. J. Cell Biol. *202*, 1107–1122.

Sabatini, D.M. (2006). mTOR and cancer: insights into a complex relationship. Nat. Rev. Cancer *6*, 729–734.

Sancak, Y., Peterson, T.R., Shaul, Y.D., Lindquist, R.A., Thoreen, C.C., Bar-Peled, L., and Sabatini, D.M. (2008). The Rag GTPases bind raptor and mediate amino acid signaling to mTORC1. Science *320*, 1496–1501.

Sancak, Y., Bar-Peled, L., Zoncu, R., Markhard, A.L., Nada, S., and Sabatini, D.M. (2010). Ragulator-Rag complex targets mTORC1 to the lysosomal surface and is necessary for its activation by amino acids. Cell *141*, 290–303.

Sanchez, P., De Carcer, G., Sandoval, I.V., Moscat, J., and Diaz-Meco, M.T. (1998). Localization of atypical protein kinase C isoforms into lysosome-targeted endosomes through interaction with p62. Mol. Cell. Biol. *18*, 3069–3080.

Shimobayashi, M., and Hall, M.N. (2014). Making new contacts: the mTOR network in metabolism and signalling crosstalk. Nat. Rev. Mol. Cell Biol. *15*, 155–162.

Sumimoto, H., Kamakura, S., and Ito, T. (2007). Structure and function of the PB1 domain, a protein interaction module conserved in animals, fungi, amoebas, and plants. Sci. STKE *2007*, re6.

Thomas, J.D., Zhang, Y.J., Wei, Y.H., Cho, J.H., Morris, L.E., Wang, H.Y., and Zheng, X.F. (2014). Rab1A is an mTORC1 activator and a colorectal oncogene. Cancer Cell *26*, 754–769.

Tsun, Z.Y., Bar-Peled, L., Chantranupong, L., Zoncu, R., Wang, T., Kim, C., Spooner, E., and Sabatini, D.M. (2013). The folliculin tumor suppressor is a GAP for the RagC/D GTPases that signal amino acid levels to mTORC1. Mol. Cell *52*, 495–505.

Valencia, T., Kim, J.Y., Abu-Baker, S., Moscat-Pardos, J., Ahn, C.S., Reina-Campos, M., Duran, A., Castilla, E.A., Metallo, C.M., Diaz-Meco, M.T., and Moscat, J. (2014). Metabolic reprogramming of stromal fibroblasts through p62-mTORC1 signaling promotes inflammation and tumorigenesis. Cancer Cell *26*, 121–135.

Wu, X.N., Wang, X.K., Wu, S.Q., Lu, J., Zheng, M., Wang, Y.H., Zhou, H., Zhang, H., and Han, J. (2011). Phosphorylation of Raptor by p38beta participates in arsenite-induced mammalian target of rapamycin complex 1 (mTORC1) activation. J. Biol. Chem. *286*, 31501–31511.

Yu, L., McPhee, C.K., Zheng, L., Mardones, G.A., Rong, Y., Peng, J., Mi, N., Zhao, Y., Liu, Z., Wan, F., et al. (2010). Termination of autophagy and reformation of lysosomes regulated by mTOR. Nature *465*, 942–946.

Yuan, H.X., Xiong, Y., and Guan, K.L. (2013). Nutrient sensing, metabolism, and cell growth control. Mol. Cell *49*, 379–387.

Zheng, M., Wang, Y.H., Wu, X.N., Wu, S.Q., Lu, B.J., Dong, M.Q., Zhang, H., Sun, P., Lin, S.C., Guan, K.L., and Han, J. (2011). Inactivation of Rheb by PRAK-mediated phosphorylation is essential for energy-depletion-induced suppression of mTORC1. Nat. Cell Biol. *13*, 263–272.

Cell Reports

Supplemental Information

Amino Acid Activation of mTORC1 by a PB1-Domain-Driven Kinase Complex Cascade

Juan F. Linares, Angeles Duran, Miguel Reina-Campos, Pedro Aza-Blanc, Alex Campos, Jorge Moscat, and Maria T. Diaz-Meco

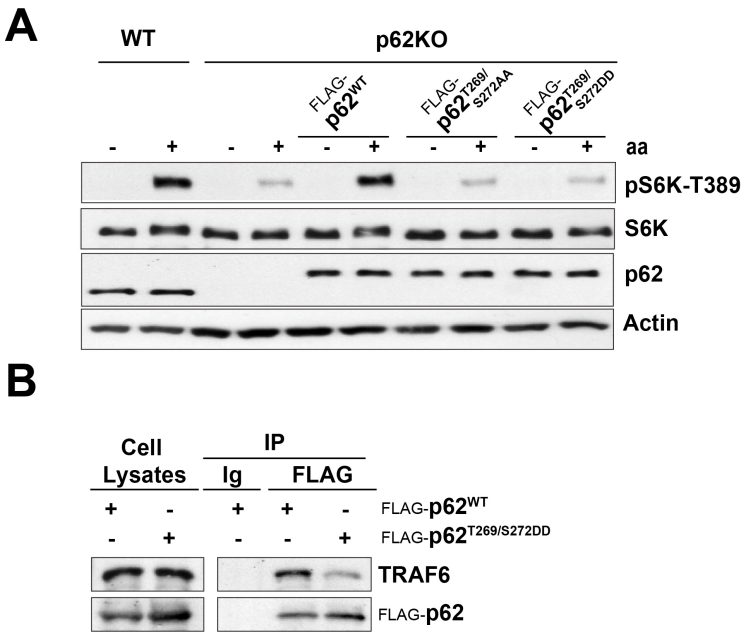

Figure S1. The Mutation of p62 Phosphorylation Sites to Aspartic Acid ,p62$^{T269/S272DD}$, Does Not Mimic p62 Phosphorylation for mTOR Activation and TRAF6 Recruitment in Response to Amino Acids, Related to Figure 1.

(A) The p62$^{T269/S272DD}$ mutant was not able to reconstitute mTOR activation in p62KO MEFs. WT and p62KO MEFs, reconstituted with p62^{WT}, p62$^{T269/S272AA}$, or p62$^{T269/S272DD}$ were starved of amino acids for 50 min and restimulated with amino acids for 20 min. Cell lysates were analyzed by western blot.

(B) The p62$^{T269/S272DD}$ mutant was not able to interact with TRAF6. HEK293T cells, transfected with the indicated plasmid were treated as in (A). Cell lysates and FLAG-tagged immunoprecipitates were immunoblotted to detect the indicated proteins.

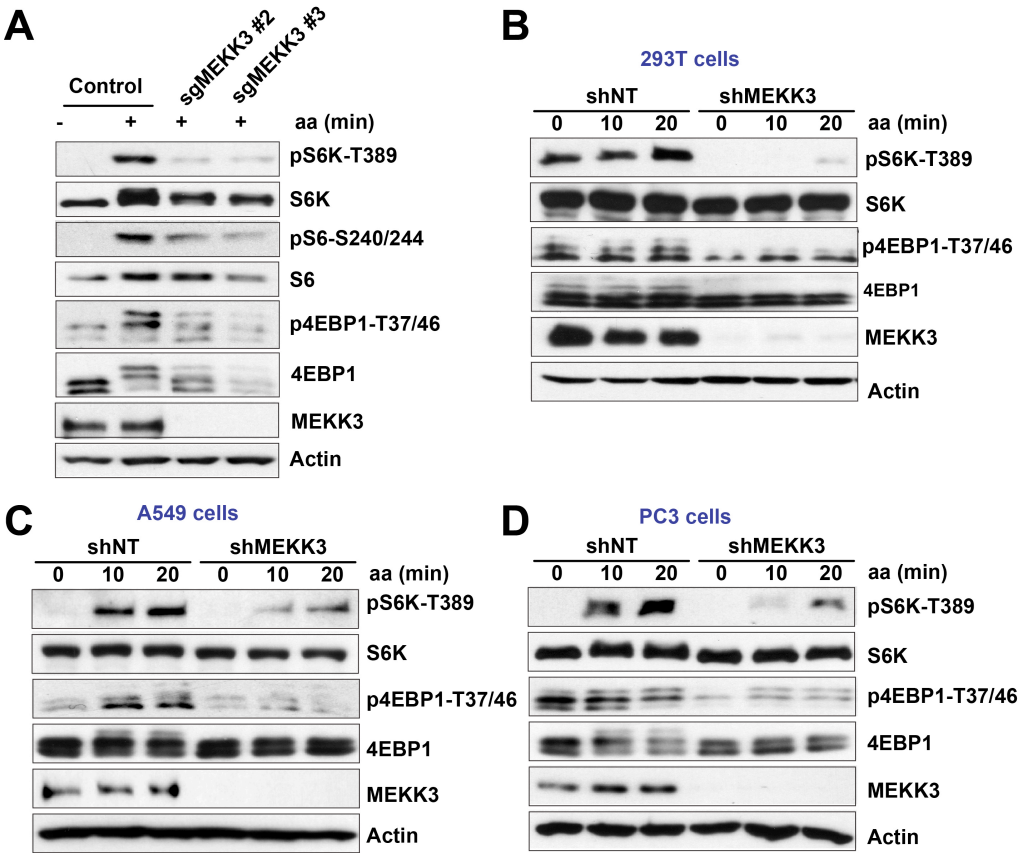

Figure S2. MEKK3 Is Required for mTORC1 Activation in Response to Amino Acids ,Related to Figure 2.

(A) MEKK3 is required for mTOR activation by amino acids. Control or MEKK3-deficient HEK293T cells were deprived of amino acids and serum for 50 min and then stimulated with amino acids for 15 min. Cell lysates were immunoblotted for the specified proteins.

(B) MEKK3 is required for mTOR activation by amino acids. shNT or shMEKK3 HEK293T cells were treated as in (A) and cell lysates were immunoblotted for the specified proteins.

(C-D) MEKK3 is required for mTOR activation by amino acids in different cell lines. shNT or shMEKK3 A549 cells and PC3 cells were treated as in (A), and immunoblotted for the specified proteins.

Results are representative of three experiments.

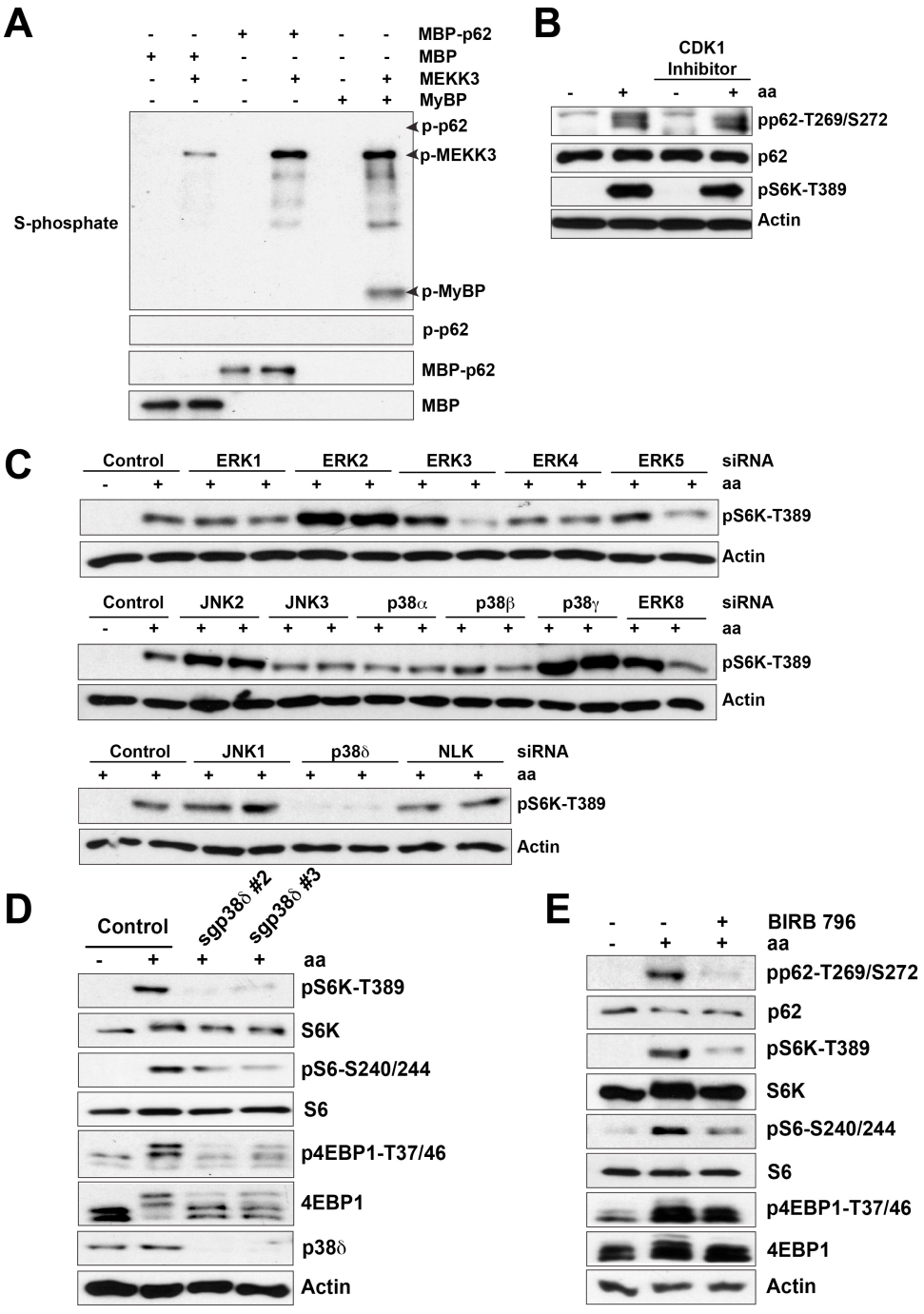
A
MBP-p62
MBP
MEKK3
MyBP
p-p62
p-MEKK3
S-phosphate
p-MyBP
p-p62
MBP-p62
MBP
B
CDK1 Inhibitor
aa
pp62-T269/S272
p62
pS6K-T389
Actin
C
Control
ERK1
ERK2
ERK3
ERK4
ERK5
siRNA
aa
pS6K-T389
Actin
Control
JNK2
JNK3
p38α
p38β
p38γ
ERK8
siRNA
aa
pS6K-T389
Actin
Control
JNK1
p38δ
NLK
siRNA
aa
pS6K-T389
Actin
D
Control
sgp38δ #2
sgp38δ #3
aa
pS6K-T389
S6K
pS6-S240/244
S6
p4EBP1-T37/46
4EBP1
p38δ
Actin
E
BIRB 796
aa
pp62-T269/S272
p62
pS6K-T389
S6K
pS6-S240/244
S6
p4EBP1-T37/46
4EBP1
Actin

Figure S3. p38δ Is Required for mTORC1 Activation and p62 Phosphorylation in Response to Amino Acids, Related to Figure 3.

(A) MEKK3 does not phosphorylate p62 in an in vitro phosphorylation assay with ATPγS.

(B) CDK1 does not phosphorylate p62 in response to amino acids. HEK293T cells, in the presence or absence of purvalanol, were deprived of amino acids for 50 min and then stimulated with amino acids for 20 min. Cell lysates were immunoblotted for the specified proteins.

(C) p38δ is required for mTOR activation by amino acids. HEK293T cells transfected with scramble siRNA or the different MAPK siRNAs were treated as in (B) and cell lysates were then immunoblotted for the specified proteins.

(D) p38δ is required for mTOR activation by amino acids. Control or p38δ-deficient HEK293T cells were treated as in (B) and cell lysates were immunoblotted for the specified proteins.

E) Inhibition of p38 enzymatic activity blocks p62 phosphorylation and mTOR activation by amino acids. HEK293T cells, in the presence or absence of the p38 inhibitor BIRB 796 (10 μM), were treated as in (B). Cell lysates were immunoblotted for the specified proteins

Results are representative of three experiments.

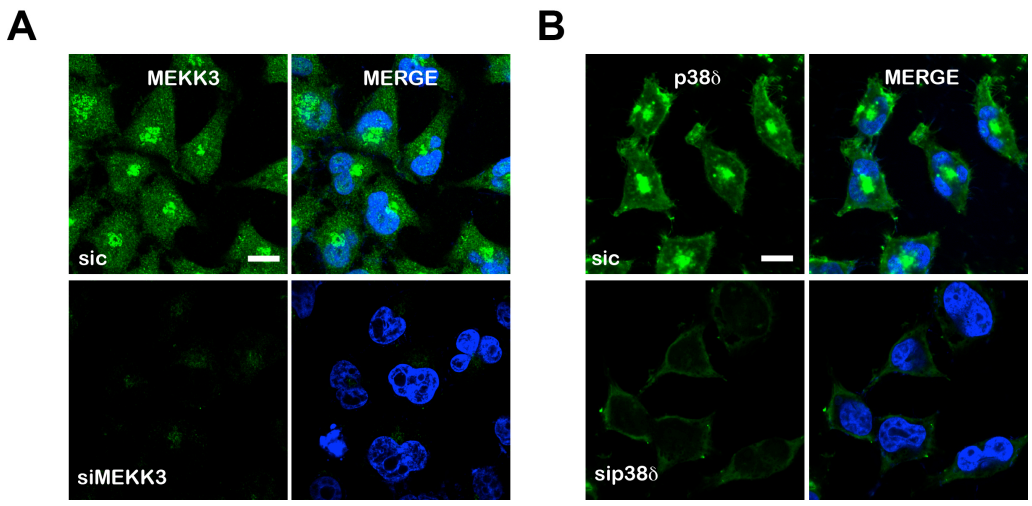

Figure S4. Antibodies Validation for Immunofluorescence, Related to Figure 4.

(A-B) Images of HeLA cells, transfected with scramble siRNA or MEKK3 or p38δ siRNA, coimmunostained for MEKK3 or p38δ and DAPI. Cells were starved for 50 min before processing. Scale bars= 10μm.

Images are representative of two independent experiments.

Supplemental Experimental Procedures

Generation of Knockout Cell Lines

The guide sequences targeting Exon 1 of human MEKK3, p38δ, and p62 are shown below.

MEKK3: 5'- GAACTCAATCATGAACGATC

p38δ: 5'- G TACGTGTCCCCGACGCACGT

p62: 5'-GAAGATCGCCTTGGAGTCCG

The single guide RNAs in the PX458 vector (4μg) were transfected into HEK293T cells using Lipofectamine 2000 according to manufacturer's instructions. 24 hours post transfection, the cells were trypsinized, washed with PBS, and re-suspended in DMEM with 2% FBS and penicillin/streptomycin. GFP-positive cells were single-sorted by FACS (Sanford-Burnham Medical Research Institute FACS core, FACS ARIA) into 96-well plates in DMEM containing 20% FBS and 50μg ml^{-1} penicillin/streptomycin. Single clones were expanded and screened for MEKK3, p38δ, and p62 by protein immunoblotting.

Antibodies and Reagents

Reagents were obtained from the following sources: primary antibodies to HA tag (sc-805), GST tag (sc-138), and Myc tag (sc-40), S6K1 (sc-230), MEKK3 (sc-28769), p38δ (sc-7585), ubiquitin (sc-8017), TRAF6 (sc-7221), and actin (sc-1616); HRP-labeled anti-mouse, anti-mouse IgG1, and anti-goat secondary antibodies were from Santa Cruz Biotechnology. Antibodies to raptor (#2280), phospho-T389 S6K1 (#9205), mTOR (#2983), phospho-T37/46 4EBP1 (#2855), 4EBP1 (#9644), AKT (#9272), phospho-S473 AKT (#4058), LC3 (#4108), phosho-Ser240/244 S6 (#5364), S6 (#2317), and HRP-labeled anti-rabbit secondary antibody were from Cell Signaling Technology. Antibody to

phospho-T269/S272 p62 was from Phospho Solutions. Antibody to LAMP2 (ab25631) was from Abcam, and to human p62 (#610833) from BD biosciences. FLAG antibody (F1804), human recombinant insulin, bafilomycin A1, purvalanol, protein A-sepharose, bovine insulin, RPMI 1640 medium, Y-27632, leucine, and 50x amino acid solution were from Sigma Aldrich. BIRB 796 was from Millipore. DMEM and fetal bovine serum were from Hyclone; FuGENE 6 and Complete Protease Cocktail were from Roche. Alexa 488-, Alexa 555-, and Alexa 568-conjugated secondary antibodies, Lipofectamine 2000, and tyramide signal amplification kits, B27, and Glutamax were from Life Technologies. RPMI 1640 medium modified to be without amino acids was from US Biological; protein G-Sepharose was from Amersham; collagenase type II, DMEM, ADMEM/F12 and TrypLE from GIBCO; EGF 5, R-spondin1, recombinant Noggin from Preprotech; growth factor-reduced Matrigel from Corning; and A83-01 from Tocris.

Isolation and Culture of Prostate Epithelial Cells

Prostate epithelial cells were prepared as previously described (Karthaus et al., 2014) with a few modifications**.** Murine prostates were isolated from 8-week-old $PTEN^{fl/fl}$-PBcre male mice and were placed in 5 mg ml^{-1} collagenase type II in ADMEM/F12 and digested for 1 to 2 h at 37°C. Glandular structures were washed with ADMEM/F12 and centrifuged at 100 G. Subsequently, structures were digested in 5 ml TrypLE with the addition of Y-27632 to 10 µM for 15 min at 37°C. Trypsinized cells were washed and seeded in growth factor-reduced Matrigel. Murine prostate epithelial cells were cultured in ADMEM/F12 supplemented with B27, 10 mM HEPES, Glutamax, and penicillin/streptomycin and containing the following growth factors: EGF 50 ng/ml, R-spondin1-conditioned medium or 500 ng/ml recombinant R-spondin1, 100 ng/ml recombinant Noggin, and the TGF-β/Alk inhibitor A83-01. Murine prostate organoids were passaged either via trituration with a glass Pasteur pipet or trypsinization with

TrypLE for 5 min at 37°C. Lentiviral infections were performed as described previously (Koo et al., 2012) using pLKO.1-puro targeting p62, MEKK3, p38δ, or control scramble. In short, 100,000 single cells were infected with an MOI $1*10^3$. Infection was done during centrifugation for 1 h at 600 G RT. Cells were subsequently placed at 37°C, 5% CO_2 for 3 h to recover. Cells were plated in Matrigel and, 24 h post seeding, 1 µg/ml puromycin was applied for 2 days to ensure only infected cells remained.

Cell Culture

HEK293T, PC3, and A549 cells were from ATCC. p62 KO MEFs were previously described (Duran et al., 2011). Cells were tested for mycoplasma contamination. Cells were cultured in DMEM with 10% FBS. For co-transfection experiments, 0.9 million HEK293T cells were plated in 6 cm culture dishes. 24 hours later, cells were transfected with 500 ng of the expression plasmids. Empty vector was added to transfection mixes to bring the total DNA quantity up to 2 µg. For amino acid starvation, HEK293T cells in 10 cm culture dishes or on coated glass cover slips were rinsed with PBS and incubated in serum and amino acid-free RPMI for 50 minutes. MEFs, PC3, and A549 cells were treated similarly, but starved for 4 hours. Cells were stimulated with a 1X amino acid mixture for different durations, as indicated. After stimulation, the final concentration of amino acids in the media was the same as in RPMI. For insulin stimulation, HEK293T cells were deprived of serum for 24 h and stimulated with 150 nM of insulin. Cells were processed for biochemical or immunofluorescence assays as described below. Cell viability was determined by Trypan Blue exclusion at the indicated times.

Plasmids

pCMV-FLAG-p62, pWZL-Hygro-p62, and pCDNA3-myc-p62 vectors have been described previously (Duran et al., 2011). pCMV-FLAG-p62 T269A/S272A, pCMV-FLAG-p62 T269D/S272D, pWZL-Hygro-p62 T269A/S272A, pCDNA3-myc-p62 D69A/D73A, pCDNA3-FLAG-p38δ T180A/Y182F plasmids were generated by in vitro mutagenesis. The following plasmids were from Addgene: Addgene plasmid 19301, pRK5-HA GST RagBGTP (Sancak et al., 2008); Addgene plasmid 20785, pCDNA3 FLAG-p38δ (Enslen et al., 2000), Addgene plasmid 12186, pCMV5 HA-MEKK3 (Blank et al., 1996); Addgene plasmid 14671, pRc/RSV FLAG MKK3 (Derijard et al., 1995), and Addgene plasmid 22418: mCherry-EGFP-LC3 (Pankiv et al., 2007).

Mammalian Lentiviral shRNAs, siRNAs, and Retroviral Transduction

TRC lentiviral shRNAs targeting human MEKK3 (TRCN0000010692, TRCN0000002305), human p38δ (TRCN0000055428), mouse MEKK3 (TRCN0000025250), mouse p62 (TRCN0000098616) and mouse p38δ (TRCN0000023092) were obtained from Sigma. shRNA-encoding plasmids were co-transfected with psPAX2 (Addgene; plasmid 12260) and pMD2.G (Addgene; plasmid 12259) packaging plasmids into actively growing HEK293T cells by using FuGENE 6 transfection reagent. Virus-containing supernatants were collected 48 hours after transfection, filtered to eliminate cells, and then used to infect target cells in the presence of 8 μg/ml polybrene. Cells were analyzed on the third day after infection. For MAPK siRNA screening, two pools of four siRNAs against each target from two different sources (Dharmacon and Ambion) were used. siRNAs were co-transfected into actively growing cells by using Lipofectamine transfection reagent. Cells were analyzed on the second day after transfection. Retroviruses were produced in Phoenix cells by transient

transfection using Lipofectamine. Culture supernatants were collected 24, 48, and 72 h post-transfection, filtered, and supplemented with 8 μg/ml polybrene. Cells were infected with three rounds of viral supernatants and selected with hygromycin (75 μg/ml).

Cell Lysis, Immunoprecipitation, Fractionation, and Immunoblotting

Cells were rinsed once with ice-cold PBS and lysed in ice-cold lysis buffer (40 mM HEPES [pH 7.4], 120 mM NaCl, 1 mM EDTA, 10 mM pyrophosphate, 10 mM glycerophosphate, and 0.3% CHAPS, and one tablet of EDTA-free protease inhibitors [Roche] per 25 ml). The soluble fractions of cell lysates were isolated by centrifugation at 13,000 rpm for 15 minutes. For immunoprecipitations, primary antibodies were added to the lysates and incubated with rotation overnight at 4°C. 40 μl of a 50% slurry of protein G-sepharose or protein A-sepharose was then added and the incubation was continued for an additional 1 hour. Immunoprecipitates were washed three times with lysis buffer. Fractionation of lysates into heavy membrane and light membrane/cytosolic fractions was performed as described (Menon et al., 2014), In brief, HEK293T cells from two near-confluent 15-cm dishes per treatment were washed with cold PBS, scraped into cold PBS, pelleted by centrifugation at 800 g for 2 min at 4°C, and re-suspended in 300 μl cold hypotonic lysis buffer (10 mM HEPES, pH 7.2, 10 mM KCl, 1.5 mM $MgCl_2$, 20 mM NaF, 100 μM sodium orthovanadate, 250 mM sucrose, with freshly added protease inhibitors). Cells were mechanically lysed by drawing 4 times through a 23G needle and then centrifuged at 500 g for 10 min at 4°C, yielding a post-nuclear supernatant (PNS). The PNS was centrifuged at 20,000 g for 2 hr to separate the soluble supernatant (light membrane/cytosolic fraction) from the insoluble pellet (heavy membrane fraction). The pellet was resuspended in RIPA buffer (40 mM HEPES, pH 7.4, 120 mM NaCl, 1 mM EDTA, 1% Triton X-100, 0.1% SDS, 1% Na deoxycholate, 5% glycerol, 10 mM sodium pyrophosphate, 10 mM glycerol 2-phosphate, 50 mM NaF,

0.5 mM sodium orthovanadate, and 1:100 protease inhibitors). Cell extracts or immunoprecipitated proteins were denatured by the addition of 20 μl of sample buffer and boiling for 5 minutes, resolved by 8%–14% SDS-PAGE, and then transferred to nitrocellulose-ECL membranes (GE Healthcare). The immune complex was detected by chemiluminescence (Thermo Scientific).

In Vitro Kinase-Assay and MS/MS Phosphopeptide Identification

For in vitro phosphorylation assays, 1 μg of recombinant MBP-p62 was incubated at 30 ºC for 60 min in kinase assay buffer containing 25 mM Tris-HCl (pH 7.5), 5 mM $MgCl_2$, 0.5 mM EGTA, 1 mM DTT, and 100 μM ATP in the presence of recombinant MEKK3 or p38δ. For ATP analog-based phosphorylation detection, the protocol described previously (Allen et al., 2007) was followed with minor modifications. Briefly, 100 μM of ATPγS (Biolog) was added to the reaction, after which PNBM (Abcam) and EDTA were added to a final concentration of 2.5 mM and 20 mM, respectively, and incubated for 1 h at room temperature. Immunoblotting detection was performed with anti-thiophosphate ester antibody from Cell Signaling. Protein digestion, TiO2-based phosphopeptide enrichment, electrospray ionization-liquid chromatography tandem mass spectrometry, and MS/MS analysis were performed as described previously (Ma et al., 2013).

Ubiquitin Detection Assay

Detection of endogenous in vivo mTOR ubiquitination was performed as described (Xiong et al., 2009). In brief, HEK293T cells were lysed with cell lysis buffer (2% SDS, 150 mM NaCl, 10 mM Tris-HCl, pH 8.0, with 2mM sodium orthovanadate, 50 mM sodium fluoride, and protease inhibitors). Cell lysates were boiled for 10 min to dissociate protein-protein interactions. The samples were diluted with dilution buffer (10

mM Tris-HCl [pH 8.0], 150 mM NaCl, 2 mM EDTA, 1% Triton). The diluted samples were incubated at 4°C for 60 min with rotation and then centrifuged for 30 min. Cell lysate was incubated with mTOR antibody overnight, after which Protein A beads were added for an additional 1 h. Immunoprecipitates were washed with washing buffer (10 mM Tris-HCl, pH 8.0, 1 M NaCl, 1 mM EDTA, 1% NP-40). Proteins were eluted in SDS-sample buffer, subjected to SDS-PAGE, transferred to nitrocellulose membrane, and immunoblotted with anti-ubiquitin.

Histological Analysis

Prostate organoids and prostates from 10-month-old $PTEN^{+/-}$ male mice were isolated, rinsed in ice-cold PBS, fixed in 10% neutral buffered formalin for 24 h, dehydrated, and embedded in paraffin. Sections (5 μm) were stained with hematoxylin and eosin (H&E). For immunohistochemistry, sections were deparaffinized, rehydrated, and then treated for antigen retrieval. After blocking in avidin/biotin solutions (Vector Laboratories), tissues were incubated with primary antibody overnight at 4 °C, followed by incubation with biotinylated secondary antibody. Endogenous peroxidase was quenched in 3% H_2O_2 in water at room temperature. Antibodies were visualized with avidin/biotin complex (Vectastain Elite; Vector Laboratories) using diaminobenzidine as the chromagen. Human prostate tissue microarray (TMA) slides were obtained from US Biomax. Stained TMA slides were scanned by using the Scanscope XT system (Aperio) and images were captured using the Aperio ImageScope software (v11.1.2.760). For the quantitative analysis, a Histo-score (H score) was calculated based on the staining intensity and percentage of stained cells using the Aperio ScaScope systems.

Immunofluorescence Assays and Colocalization Measurements

HeLa, HEK293T, and A549 cells were plated on fibronectin-coated glass coverslips in 24-well tissue culture plates. 24 hours later, cells were amino acid starved, and then stimulated with amino acids as described above, rinsed with PBS once, fixed with warmed 4% formaldehyde, and permeabilized with 0.1% Triton X-100. Fixed cells on cover slips or sections from human prostate samples, previously deparaffinized, were blocked for one hour in blocking buffer (0.3% BSA in PBS) and then incubated with primary antibody in blocking buffer overnight at 4°C. Samples were then rinsed twice with blocking buffer and incubated with secondary antibodies for one hour at room temperature in the dark, followed by tyramide signal amplification. Slides were mounted on Mowiol and examined with a FluoView 1000 Olympus Laser Point Scanning Confocal Microscope. The colocalization plugin in ImageJ (NIH) was applied to measure co-localization between two channels of confocal z stacks (a constant threshold for all the images within each experiment was applied). A maximum-intensity projection was generated, and the area of co-localizing pixels was quantified using the JACoP plugin in ImageJ, and expressed as the total area of colocalization per cell. Quantification was carried out on at least 15 cells per condition from two independent experiments.

Cell-Size Determinations

For measurement of cell size, triplicates of each sample were analyzed using Countess Automated cell counter (Invitrogen).

Supplemental References

Allen, J.J., Li, M., Brinkworth, C.S., Paulson, J.L., Wang, D., Hubner, A., Chou, W.H., Davis, R.J., Burlingame, A.L., Messing, R.O.*, et al.* (2007). A semisynthetic epitope for kinase substrates. Nat Methods *4*, 511-516.

Blank, J.L., Gerwins, P., Elliott, E.M., Sather, S., and Johnson, G.L. (1996). Molecular cloning of mitogen-activated protein/ERK kinase kinases (MEKK) 2 and 3. Regulation of sequential phosphorylation pathways involving mitogen-activated protein kinase and c-Jun kinase. J Biol Chem *271*, 5361-5368.

Derijard, B., Raingeaud, J., Barrett, T., Wu, I.H., Han, J., Ulevitch, R.J., and Davis, R.J. (1995). Independent human MAP-kinase signal transduction pathways defined by MEK and MKK isoforms. Science *267*, 682-685.

Duran, A., Amanchy, R., Linares, J.F., Joshi, J., Abu-Baker, S., Porollo, A., Hansen, M., Moscat, J., and Diaz-Meco, M.T. (2011). p62 is a key regulator of nutrient sensing in the mTORC1 pathway. Mol Cell *44*, 134-146.

Enslen, H., Brancho, D.M., and Davis, R.J. (2000). Molecular determinants that mediate selective activation of p38 MAP kinase isoforms. EMBO J *19*, 1301-1311.

Karthaus, W.R., Iaquinta, P.J., Drost, J., Gracanin, A., van Boxtel, R., Wongvipat, J., Dowling, C.M., Gao, D., Begthel, H., Sachs, N.*, et al.* (2014). Identification of multipotent luminal progenitor cells in human prostate organoid cultures. Cell *159*, 163-175.

Koo, B.K., Stange, D.E., Sato, T., Karthaus, W., Farin, H.F., Huch, M., van Es, J.H., and Clevers, H. (2012). Controlled gene expression in primary Lgr5 organoid cultures. Nat Methods *9*, 81-83.

Ma, L., Tao, Y., Duran, A., Llado, V., Galvez, A., Barger, J.F., Castilla, E.A., Chen, J., Yajima, T., Porollo, A.*, et al.* (2013). Control of Nutrient Stress-Induced Metabolic Reprogramming by PKCzeta in Tumorigenesis. Cell *152*, 599-611.

Menon, S., Dibble, C.C., Talbott, G., Hoxhaj, G., Valvezan, A.J., Takahashi, H., Cantley, L.C., and Manning, B.D. (2014). Spatial control of the TSC complex integrates insulin and nutrient regulation of mTORC1 at the lysosome. Cell *156*, 771-785.

Pankiv, S., Clausen, T.H., Lamark, T., Brech, A., Bruun, J.A., Outzen, H., Overvatn, A., Bjorkoy, G., and Johansen, T. (2007). p62/SQSTM1 binds directly to Atg8/LC3 to facilitate degradation of ubiquitinated protein aggregates by autophagy. J Biol Chem *282*, 24131-24145.

Sancak, Y., Peterson, T.R., Shaul, Y.D., Lindquist, R.A., Thoreen, C.C., Bar-Peled, L., and Sabatini, D.M. (2008). The Rag GTPases bind raptor and mediate amino acid signaling to mTORC1. Science *320*, 1496-1501.

Xiong, H., Wang, D., Chen, L., Choo, Y.S., Ma, H., Tang, C., Xia, K., Jiang, W., Ronai, Z., Zhuang, X.*, et al.* (2009). Parkin, PINK1, and DJ-1 form a ubiquitin E3 ligase complex promoting unfolded protein degradation. J Clin Invest *119*, 650-660.

Cell Research (2015) 25:537-538.
© 2015 IBCB, SIBS, CAS All rights reserved 1001-0602/15 $ 32.00
www.nature.com/cr

RESEARCH HIGHLIGHT

Nutrient stress revamps cancer cell metabolism

Cell Research (2015) **25**:537-538. doi:10.1038/cr.2015.38; published online 31 March 2015

Efforts to identify new therapeutic targets in cancer primarily focused on oncogenes and tumor suppressor genes, and their mechanisms of action. However, there is an emerging alternative strategy that involves identification of target proteins that are not encoded by oncogenes, but are, nonetheless, required to accommodate cancer-specific stresses.

One of the most interesting, and possibly richest, sources for new therapeutic targets is the cellular machinery regulating cancer cell metabolism. Tumor cells normally rely on aerobic glycolysis to maintain cell growth and proliferation, even in the presence of normal concentrations of oxygen [1]. This paradoxical situation makes cancer cells relatively resistant to growth inhibition in conditions of oxygen deprivation, and provides a way to rapidly produce the cellular energy and metabolites required for the high rate of anabolism that drives the dramatically increased proliferation of cancer cells [1]. This is an efficient metabolic mechanism as long as cancer cells have access to a constant supply of glucose. However, cancer cell addiction to a high glucose supply makes them vulnerable and, therefore, susceptible to nutrient stress. Notably, nutrient deprivation has been correlated with poor patient survival [2], suggesting that instead of killing the tumor, the scarcity of nutrients can make the cancer cell stronger. This is likely because the existence of biochemical alterations that allow cancer cells to acquire the plasticity necessary to reprogram their metabolism in response to different nutrient conditions, positioning them better to compete, and thus resulting in a more aggressive tumor. In this regard, the work of Sun and co-workers show that when cancer cells are deprived of glucose or glutamine, the serine biosynthesis pathway (SSP) is activated [3] (Figure 1). These results confirm previous data in colon cancer cells demonstrating that glucose deprivation promotes cell death unless they are deficient in the atypical PKC, PKCζ, and thus they can synthesize serine and glycine from glutamine through a process of "reverse glycolysis" [4]. Interestingly, Sun *et al*. [3] extended these observations and made the important finding that the SSP pathway is activated not only under glucose deprivation condition [4] but also when cells are deprived of glutamine. These observations begged the question, why is the SSP pathway so relevant? The first evidence of the importance of this pathway for tumorigenesis came from the studies of Locasale and co-workers who found that certain cancer cells utilize part of the glycolytic carbon for the serine biosynthetic pathway, which correlated with the amplification of phosphoglycerate dehydrogenase (PHGDH; Figure 1) [5]. Consistent with these data, it was also shown that cell proliferation was severely attenuated by downregulation of PHGDH in cells with an amplified *PHGDH* gene [5]. This suggests that the channeling of glycolytic products to this pathway might have a number of metabolic benefits that cannot be compensated by the import of extracellular serine. Interestingly, Possemato *et al*. [6] also established the 3-phosphoglycerate (3PG) → serine pathway as relevant to cancer, and suggested that the production of α-ketoglutarate from glutamine-derived glutamate during the conversion of phospho-hydroxypyruvate to phospho-serine by PSAT1 was the relevant step for tumorigenesis (Figure 1). More recent data demonstrated that serine-driven one-carbon metabolism, in which oxidation of methylene tetrahydrofolate to 10-formyl-tetrahydrofolate is coupled to reduction of $NADP^+$ to NADPH, is a source of reducing potential with comparable importance to the oxidative pentose phosphate pathway [7]. This pathway also supports another critical component of the cellular redox system, glutathione biosynthesis, as glycine is one of the three amino acids (along with glutamate and cysteine) that compose glutathione. This could explain at least in part why the SSP cascade is so relevant and, according to the recent evidences, so heavily regulated.

In this regard, two very recent studies further support this notion. Gottlieb and co-workers have recently demonstrated that serine is a natural ligand of pyruvate kinase M2 (PKM2), and that serine binding allosterically activates PKM2 enzymatic activity [8]. This has important metabolic implications due to the critical role played by PKM2 in the regulation of the glycolytic flux (Figure 1). Furthermore, Thompson and co-workers presented compelling evidence that PKM2 exerts a regulatory contribution to the serine synthetic pathway [9]. Thus, in the absence of serine, the glycolytic flux to lactate is diminished due to the reduced activity of PKM2, which results in the accumulation of glycolytic intermediates that are diverted to the PHGDH-driven serine biosynthetic pathway [9]. This model implies that cancer cells, by express-

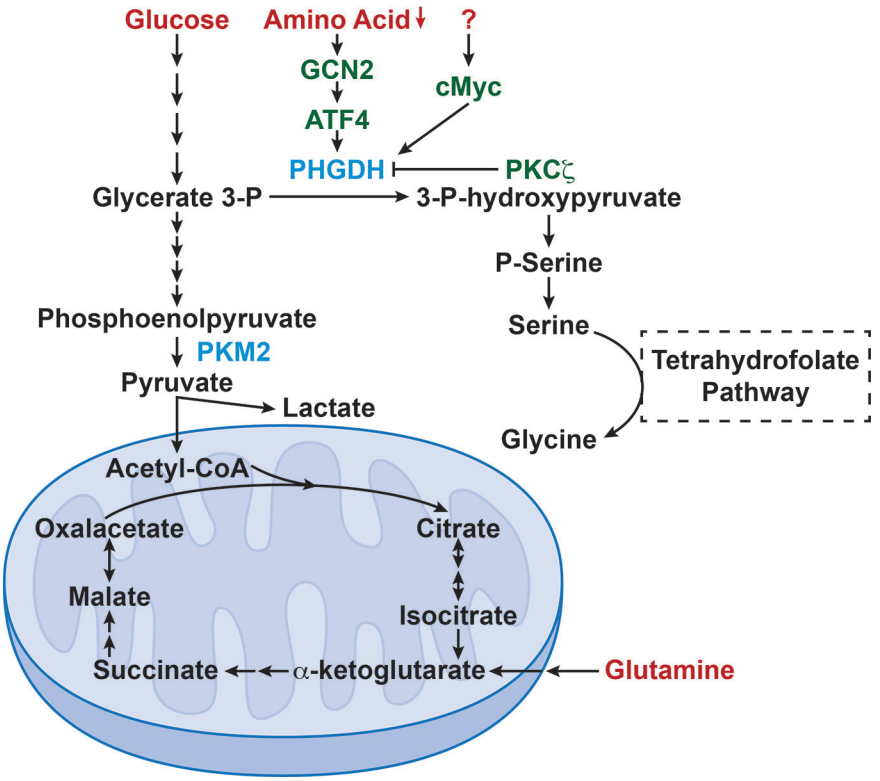

Figure 1 Nutrient sensing and stress in the serine pathway.

ing PKM2, can maintain high levels of anabolism and cell proliferation in the absence of serine in the extracellular milieu. Therefore, the crosstalk between PHGDH and PKM2 appears central to the regulation of cancer metabolism. The results of Sun *et al*. [3] showing that c-Myc stimulated SSP activation by transcriptionally regulating the expression of several SSP enzymes in cancer cells adds another very interesting layer of complexity to the regulation of the pathway. However, much work remains to be done to fully understand this complex regulatory cascades and their relevance in cancer metabolism. For example, it is clear that PHGDH, a critical enzyme in the SSP cascade, is doubly repressed by PKCζ at the transcriptional level and by phosphorylation, which again is consistent with the relevance of this pathway [4]. How this fits with the activation of c-Myc needs to be clarified. In the same vein, the SSP cascade is also controlled by a GCN2 → ATF4 module that acts as a sensor of the extracellular levels of amino acids and that is important for mTORC1 activation [9]. Key questions that remain to be addressed are how nutrient stress regulates c-Myc to impact PHGDH in the context of ATF4 activation and PKCζ activity. Furthermore, recent data from Valencia *et al*. [10] demonstrated that the downregulation of c-Myc in p62/mTORC1-deficient stromal fibroblasts results in impaired SSP that leads to more ROS and inflammation, which creates a more protumorigenic microenvironment in prostate cancer and likely in other tumors. This is important to consider because therapies aimed at blocking c-Myc or mTORC1 at a systemic level will create a more reactive tumor stroma that will likely hamper the therapeutic efficacy of these treatments in the tumor epithelium.

Jorge Moscat[1], Adam Richardson[1], Maria T Diaz-Meco[1]

[1]*Sanford-Burnham Medical Research Institute, La Jolla, CA 92037, USA*
Correspondence: Jorge Moscat
E-mail: jmoscat@sanfordburnham.org

References

1 Vander Heiden MG, Cantley LC, Thompson CB. *Science* 2009; **324**:1029-1033.
2 Le QT, Chen E, Salim A, *et al*. *Clin Cancer Res* 2006; **12**:1507-1514.
3 Sun L, Song L, Wan Q, *et al*. *Cell Res* 2015; **25**:429-444.
4 Ma L, Tao Y, Duran A, *et al*. *Cell* 2013; **152**:599-611.
5 Locasale JW, Grassian AR, Melman T, *et al*. *Nat Genet* 2011; **43**:869-874.
6 Possemato R, Marks KM, Shaul YD, *et al*. *Nature* 2011; **476**:346-350.
7 Fan J, Ye J, Kamphorst JJ, *et al*. *Nature* 2014; **510**:298-302.
8 Chaneton B, Hillmann P, Zheng L, *et al*. *Nature* 2012; **491**:458-462.
9 Ye J, Mancuso A, Tong X, *et al*. *Proc Natl Acad Sci USA* 2012; **109**:6904-6909.
10 Valencia T, Kim JY, Abu-Baker S, *et al*. *Cancer Cell* 2014; **26**:121-135.